WPCA NEWS
Worldwide Pollution Control Association
www.wpca.info
A Bi-Annual Newsletter Sponsored by the WPCA Winter - 2011

Executive Summary

The Evolution of FGD Equipment Design and Operating Practices has Changed the Conditions that FGD Materials of Construction (MOC) Must Survive

By Ron Richard, RE Consulting

Since the original design of the first FGD system, there has been a continuous evolution in the design based on lessons learned, cost factors, and changing environmental regulations. As these design changes have been made, the operating conditions inside the absorber towers have changed also. Some of these changes have led to failures of materials of construction that had previously worked well. This paper chronicles the design changes that have been made and discusses their impact on the materials of construction. . ***Full Story….***

Description of a Pseudo-Particulate Formation Mechanism in New EPA Method 202

By Jack Bionda, Clean Air Engineering

This article describes a pseudo condensable particulate matter (CPM) formation mechanism in new EPA Reference Method 202. The results of recent field testing using Method 202 on a coal-fired CFB boiler which utilizes an ammonia-based selective non-catalytic reduction (SNCR) system are discussed. The results clearly show that CPM test results can be biased high as the result of the interaction of ammonia, sulfur dioxide and water in the Method 202 impingers.
Full Story….

Larger Multiple-Tube Mechanical Dust Collectors Are Not Always Better

By Chris McKeown, Babcock & Wilcox

Mechanical dust collectors are often used for particulate collection in many processes. It is often confusing as to which collecting tube size is the most efficient. This article will utilize basic principles of physics to demonstrate that centrifugal force is indirectly proportional to the radius of a collecting tube. The examples show that smaller collecting tubes produce higher centrifugal force and therefore produce higher efficiency. ***Full Story….***

A Mechanistic Study on the Inhibition of the DENOX Reaction on the Mercury Oxidation Over SCR Catalysts

By Karin Madsen, Haldor Topsoe A/S; Anker D. Jensen, Technical Institute of Denmark;
Flemming J. Frandsen, Technical Institute of Denmark; Joakim R. Thogersen, Haldor Topsoe A/S

SCR catalysts used for NOx control promote the oxidation of mercury to $HgCl_2$ in flue gases from coal-fired power plants. Oxidized mercury is water-soluble and can be captured in a wet scrubber. This means that the combination SCR + wet FGD can offer an effective control option for mercury. Unfortunately, a considerable scatter in the level of mercury oxidation over SCR reactors in full-scale is seen. In the quest of optimizing the mercury oxidation for different SCR applications, a greater fundamental understanding of the mercury chemistry over SCR catalysts is needed. Laboratory experiments have been carried out at Haldor Topsøe A/S to elucidate and quantify the mercury oxidation over commercial SCR catalysts. Results are discussed here. ***Full Story….***

WPCA NEWS
www.wpca.info
A Bi-Annual Newsletter Sponsored by the WPCA
Winter 2011

WORLDWIDE POLLUTION CONTROL ASSOCIATION

The Evolution of FGD Equipment Design and Operating Practices has Changed the Conditions that FGD Materials of Construction (MOC) Must Survive

By Ron Richard, RE Consulting

Abstract

This paper is intended for those who are familiar with the materials of construction (MOC) that are used in utility flue gas desulfurization (FGD) systems but may not be familiar with the design details or operational practices of these systems. There has been a constant evolution of the system designs and operational practices as environmental laws change and more efficient practices are discovered.

This evolution can have profound effects on the operating environment that the MOC must be able to withstand. The relationship between pH, chloride and fluoride concentrations has a definite impact on which MOC can be successfully used. The presence or absence of deposits on the surface of the MOC can affect it performance.

This paper will describe the basic design of a FGD system, and then chronicle the changes that have occurred in arriving at the current generation of FGD systems. For each of these changes, it will focus on how the change affects the environment that the MOC is exposed to.

The Basic Design

When it was determined that the electric utility industry needed to install Flue Gas Desulfurization (FGD) Systems on their boilers, they looked to the chemical process industry to see what equipment was used to remove a gas from a stream of mixed gases. They found that vertical packed towers were used in such applications. (see Figure 1)

In a vertical packed tower, the gas stream rises vertically entering near the bottom of the tower and exiting from the top of the tower. A flow of liquid containing a chemical that will absorb the desired gas constituent flows downward through the tower. To promote a large liquid surface area for good liquid/gas contact, a bed of shaped objects is placed in the vessel for the liquid to flow over. A sump at the bottom of the tower collects the liquid which can be recirculated over the bed for maximum usage of the absorbing chemical. At the top of the tower, a mist eliminator removes any liquid aerosol particles to prevent them from leaving the tower.

The diameter of the tower was determined by the design of the mist eliminator. At this point in time, most vertical flow mist eliminators were limited to 10 feet/second gas velocity. Dividing the actual flue gas flow by 10 feet/second gave the diameter of the tower. The height

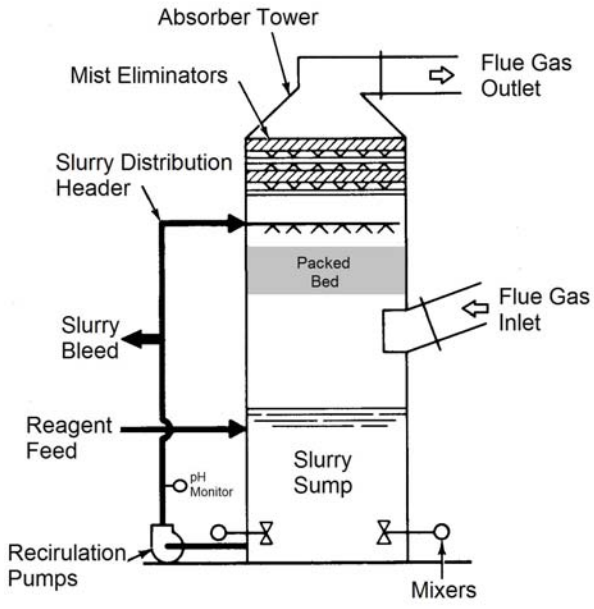

Figure 1. Packed Bed Absorber Tower

of the bed was determined by the contact time needed between the gas and the absorbent.

Liquid/Gas (L/G) ratio is a number that can quickly allow someone to compare an absorber's design. The liquid portion is the gallons per minute of absorbent being recirculated through the absorber tower. The gas portion is the actual cubic feet per minute of wet cool flue gas exiting the absorber tower expressed in units of 1000 ACFM. So the liquid/gas ratio is in units of gallons/1000 ft^3.

An absorber tower that has a recirculation flow of 10,000 GPM and a gas flow of 100,000 ACFM would have a liquid/gas ratio (10,000/100) or 100 gallons/1000 ft^3. Or in more common terms one would say the tower has an L/G of 100.

An absorber using very reactive sodium chemistry might be designed with an L/G of 10. The L/G ratio sets the size of the recirculation pumps on the tower based on the flue gas flow that will be passing through the tower. The higher the L/G, the bigger the pumps and the higher the capital costs. The operating costs will also be higher because of the higher horsepower requirements.

The diameters for the towers were quite large, so often the gas flow was divided into multiple towers of smaller diameter for each boiler. The bed materials for the original towers were marbles, ping pong balls, or egg crate packing (large crossed interlocking slats like those used to separate eggs in crates). Since SO_2 is a weak acid, it was decided to use a weak base to remove it. The original chemical chosen was soda ash (Na_2CO_3) since it was fairly cheap, readily available and allowed a low L/G ratio.

Sodium Based Operation

This first sodium based design removed SO_2 fairly efficiently. Unfortunately the resulting sodium sulfite and sodium sulfate were also water soluble, so it was impossible to separate the spent byproducts from the fresh absorbent, so a mixture of both was removed from the tower.

The next evolution was called "dual alkali" were a clarifier was added to treat the liquid leaving the absorber. Calcium was added through the addition of hydrated lime ($Ca(OH)_2$) to the liquid. The calcium reacted and converted the sodium sulfite and sodium sulfate to calcium sulfite and calcium sulfate which would then precipitate as solids to the bottom of the clarifier for removal. The unreacted soda ash would leave the top of the clarifier and be returned to the absorber tower. Unfortunately the clarifiers weren't that efficient, so significant soda ash was still lost through the bottom of the clarifier. The operating costs were lower, but still substantial.

Since everything was soluble in the absorber in sodium based operation, there were no deposits formed in the absorber. Since there was a large loss of liquid from the absorber, the chloride and fluoride levels didn't become concentrated and corrosion wasn't a severe issue with the absorber MOC.

Converting to Calcium Based Operation

The next evolution was to convert to using finely ground limestone ($CaCO_3$) or hydrated lime ($Ca(OH)_2$) as the basic reagent that reacted with the acidic SO_2 in the flue gas. Both materials were more regionally available at a much lower cost than soda ash. This lowered the operating cost substantially.

Both of these chemicals were less reactive than soda ash, requiring a larger L/G ratio to obtain the same SO_2 removal. The L/G ratio for hydrated lime was around 30 while the L/G ratio for limestone was around 60. These larger recirculation rates required larger pumps and larger diameter absorber towers to accommodate the increased liquid flows. This increased capital cost, but the operating cost savings offset this.

Another down side was that both of these materials entered the absorber as abrasive slurries of fine particles. They then reacted to form slurries of calcium sulfite and calcium sulfate. The particles of calcium sulfite and calcium sulfate grew as crystals as they recirculated in the absorber slurry. Some of the slurry could then be bled to a thickener to separate these solids from the slurry which was returned to the absorber.

But as the crystals grew in the slurry, they also grew on the tower walls and on the surfaces of the packed bed. The deposits on the tower walls lead to "under deposit" corrosion opportunities. The deposits on the bed packing led to less open area through the packed bed. This would eventually lead to choking off the liquid flow through the bed. When this happened, the old bed packing would have to be removed and new packing would be installed. The removal of the old bed packing could require jack hammers or in some extreme cases dynamite.

The hydrated lime scrubbers operated in the 6.0-6.7 pH range while the limestone scrubbers operated in the

5.4-6.0 pH range. The improved thickener operation returned more of the liquid to the absorber tower. This also returned more of the soluble chlorides and fluorides that were removed along with the SO_2 from the flue gas and their concentrations began to climb in the absorber towers. The lower pH ranges along with the higher halide values began to corrode the 304 and 316 stainless steel alloys.

The outage time required and the expense to remove and replace the packed bed pushed the tower design to the next step.

Open Spray Tower Design

The next step was the open spray tower design. (see Figure 2) In this design, the packed bed was replaced by a cloud of fine slurry droplets suspended in the vertically rising flue gas flow. The smaller the droplets, the more surface area per gallon of slurry one would obtain, but if the droplets were too small, some of the liquid would leave the absorber tower through the mist eliminator. The surface area was important because the SO_2 in the flue gas would only react with the alkali at the surface of the droplets in the short amount of time available before the droplets fell into the pool of slurry in the bottom of the absorber tower.

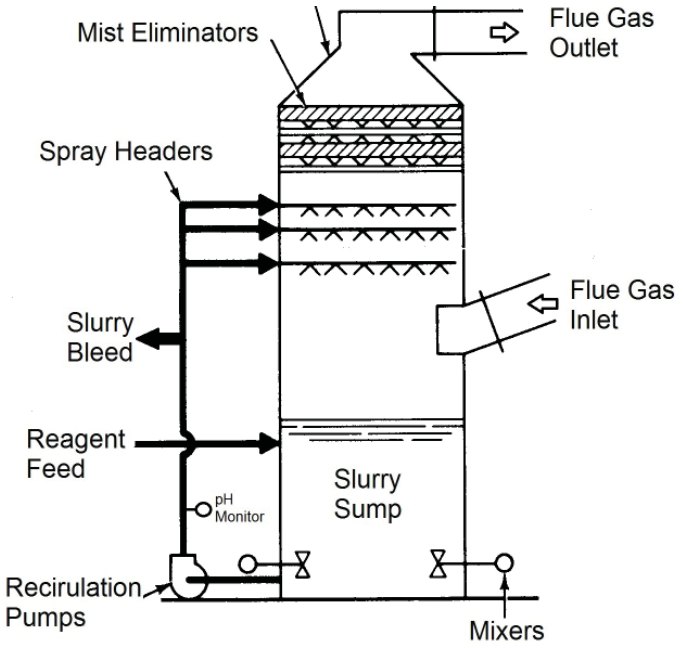

Figure 2. Spray Absorber Tower

Once the droplets fell into the pool, there was enough time to complete the reaction and form calcium sulfite and calcium sulfate. The pH was measured as the slurry passed through the recirculation pumps on its way back to the spray nozzles. Since the surface of the droplets absorbed the acidic SO_2, the pH in the upper section of the tower was actually less than what was being measured and reported. So the MOC in the upper part of the absorber tower were exposed to a slightly lower pH than what was recorded by the instrumentation.

To obtain uniform droplet coverage of the absorber tower cross section, numerous spray nozzles located on several elevations were used. It soon became apparent that the tower walls and all the slurry spray piping, piping supports and nozzles were being subjected to erosion from the constant bombardment of the solids contained in the slurry droplets. Care had to be taken in designing slurry spray patterns to protect these components from severe erosion. In some cases, erosion resistant coatings were needed to protect structural members.

So in some locations, there were areas where the erosion and lower pH were attacking the bare MOC, while at other locations the scale deposits were covering the MOC and under deposit corrosion was an issue.

Tray Tower Design

The tray tower is actually a subset of the spray towers. The only difference is that a perforated tray has been installed across the entire cross section of the tower below the spray nozzle section. The slurry droplets falling in the tower collect on the tray and must drain through the holes in the tray. The rising flue gas must also pass through these holes. The interaction between the flue gas and the slurry creates a froth layer on the tray. The surface of the bubbles in the froth provides a large surface area for the SO_2 to react with the alkalinity in the slurry. The back pressure from the tray on the flue gas causes the flue gas flow to become more evenly distributed across the cross section of the tower.

The tray doesn't change any of the corrosion properties of a spray tower.

Wet/Dry Interface

The hot flue gas enters the tower through a duct opening in the tower wall above the slurry pool and turns to flow vertically upwards through the tower. The hot gas is quenched by the falling slurry droplets to its saturation temperature.

When a slurry droplet impacts the tower wall, it adheres and forms a slurry film that runs down the wall to the slurry pool in the bottom of the tower. In the area of the wall adjacent to this duct opening, the hot gas sometimes evaporates all

the slurry from the wall leaving it dry. But just as quickly, the slurry running down the wall can cool and wet the wall again. This constant cycle of wetting and evaporation can quickly build a thick layer of deposit on the wall.

Because of the wetting/evaporation, soluble salts in the slurry can be deposited in and under this layer of deposit. Concentrations of chlorides and fluorides many times higher than those found in the slurry are found under these deposits. This area continues to be one of the most aggressive areas for MOC to survive. Many utilities will only use high nickel alloys in this area.

Pre-scrubber

Because of the corrosion issues caused by chlorides and fluorides, it seemed a good idea to remove them from the flue gas before it entered the large absorber towers. This pre-scrubber would be a much smaller diameter spray tower to quench the hot flue gas and remove the highly acidic components from the gas.

Since one desired to remove the highly acidic components and not the weakly acidic SO_2, a very low L/G ratio of slurry was used in this tower. This was effective at removing almost all of the chlorides and fluorides, but resulted in a recirculating slurry with a pH which was sometimes in the 1.0 - 3.0 range. The combination of high concentrations of chlorides and fluorides along with low pH resulted in a short life for most MOC that were tried.

Comparing the benefits of not having the chlorides and fluorides in the main absorber tower versus the cost and effort of trying to maintain the MOC in the pre-scrubber caused this idea to be abandoned at most locations.

Outlet Duct

Once the flue gas has passed through the mist eliminator, most of the slurry droplets containing the alkalinity have been removed. The flue gas is completely saturated. If the flue gas cools in the outlet duct, some water will condense and run down the walls. There is still a small amount of SO_2 in the flue gas. There is almost no alkalinity present to react with the SO_2, so some concentration of sulfuric acid will form on the walls and floors. The MOC in the outlet duct must be resistant to this sulfuric acid.

Bypass Reheat

There was a period of time when a portion of the flue gas was bypassed around the absorber tower and mixed with the clean flue gas to raise its temperature to obtain a better "plume rise" as the gas exited the top of the chimney. Of course this bypass gas had the full concentration of SO_2 exiting the boiler. After the mist eliminator, there was almost no alkalinity in the clean flue gas. This resulted in large amounts of sulfuric acid being formed and pH values in the 0.1 - 0.5 range. Most MOC failed under these conditions.

With the higher required percentage removals of SO_2 under the current environmental regulations, one can't afford to bypass any unscrubbed gas into the outlet duct. It was also found that the reheat wasn't needed as badly as people thought. So at the present time, this highly corrosive practice has ceased at most locations.

Tightening the Water Balance

The use of packing type seals on mixer and pump shafts in slurry applications required a continuous flow of fresh seal water to keep the slurry particles from getting under the packing and scoring the shafts. This fresh water traveled along the shaft and entered the absorber tower. This diluted the slurry in the absorber tower. In a large tower with multiple mixers and pumps, this freshwater flow was a significant number of gallons per minute.

At the back end of the FGD process, the calcium sulfite and calcium sulfate was removed from the process using thickeners, vacuum filters or centrifuges. Some of the liquid remained in these solids while the rest was recycled to the FGD process. The chlorides and fluorides in the liquid that remained in the solids left the FGD process, the rest returned to the process in the recycled liquid.

With improved design and operation of thickeners, vacuum filters, and centrifuges, utilities were able to obtain drier solids from the back end of the process. This meant that more chlorides and fluorides were recycled back to the absorber towers.

With the development of mechanical seals that didn't need seal water in slurry applications, the flow of fresh dilution water into the absorber towers disappeared.

Both of these developments caused the levels of chlorides and fluorides to increase in the FGD systems which led to the failure of some MOC.

Oxidation

Natural Oxidation..... When coal is burned in a large boiler, excess air is added to assure complete combustion. Then as the flue gas passes through fans, air heaters, and particulate

collection devices, oxygen enters through various leaks in seals, expansion joints and duct walls. So the flue gas entering the absorber tower has some amount of excess oxygen.

With all the problems caused by scale buildup and under deposit corrosion, EPRI funded research into the formation of calcium sulfite and calcium sulfate in the FGD system. They found that it was not unusual to find 20% - 40% of the calcium sulfite had been converted to calcium sulfate as it reacted with the naturally occurring oxygen in the flue gas.

Crystals grow best if the ions of a compound can attach themselves into the crystal matrix of an existing crystal. Calcium sulfite forms a flat rectangular crystal much like a broken pane of window glass. Calcium sulfate forms a hexagonal columnar crystal much like a broken pencil. When both types of crystals were trying to grow in the same location, they interfered with each other and formed something that under a microscope was described as a rosette, a spiny ball or a porcupine ball.

This interference in crystal growth caused the growth potential of the ions of the two compounds to backlog, causing the crystals to try to form on any surface they could find. This led to all the scale buildup seen by the FGD system operators.

The EPRI funded research found that if the percentage of calcium sulfite that was oxidized could be kept below 15%, predominately calcium sulfite crystals would grow at a rapid rate relieving the backlog of crystal growth potential and the scaling problems were greatly mitigated.

On the other hand, they found that if more than 95% of the calcium sulfite was oxidized, predominately calcium sulfate crystals would grow at a rapid rate also relieving the backlog of crystal growth potential and the scaling problems were greatly mitigated.

It was only when the FGD system was operated in the natural oxidation range that scale formation and all of its effects became an issue.

Inhibited Oxidation..... Chemists knew that sodium thiosulfate could inhibit oxidation reactions. This was tried in FGD systems with some positive effects, but the amount required made it cost prohibitive. Then it was discovered that adding a colloidal suspension of elemental sulfur to a FGD system would naturally cause thiosulfate to form as it reacted with the scrubber chemistry. This proved very cost effective in obtaining the high levels needed to keep the sulfite oxidation below the 15% level.

Several utilities switched to this mode of operation and reported minimal scale formation issues in their towers. This also eliminated most of the under deposit corrosion issues they had been dealing with. The chemistry in the absorber tower was in a reducing mode with measured ORP values several hundred mV on the negative side of the range.

Forced Oxidation..... If air is sparged through the scrubber slurry in large volumes, all the calcium sulfite can be oxidized to calcium sulfate. When this was done, utilities reported minimal scale formation issues in their towers. This also eliminated most of the under deposit corrosion issues they had been dealing with. The chemistry in the absorber tower was in an oxidizing mode with measured ORP values several hundred mV on the positive side of the range.

Another benefit is that the calcium sulfate (gypsum) can be sold to make drywall or for agricultural use. These markets were rather slow at first, but now large amounts of this gypsum are being sold with the proceeds from these sales offsetting some of the FGD system operating costs.

External Oxidation..... In this mode, there are no changes made in the absorber tower. An external oxidation tank is erected. The waste bleed stream is routed to this oxidation tank where the air is sparged through the slurry at a pH in the 4 - 5 range. The tank can be designed for the optimum growth of the gypsum crystals.

One disadvantage of this mode is that the absorber tower is still operating in the natural oxidation mode. This means it is still having scaling problems. Another disadvantage is that this mode requires additional tanks, pumps and mixers. This is a large additional capital expense.

In-situ Oxidation..... It was discovered that if the air was sparged into the absorber tower, the slurry was sufficiently oxidized although not as efficiently as in the external oxidizer. The advantage, however, was that there was no additional tanks, pumps and mixers and the absorber tower now reaped the advantage of forced oxidation with minimal scaling issues in the absorber tower.

This mode of operation has become the standard design in the latest generation of FGD absorbers. If one is selling the gypsum to a wall board plant, they will pay a premium if there is a minimal amount of calcium sulfite or calcium car-

bonate mixed with the gypsum. So there is a benefit to running an excess amount of air to assure complete oxidation of the calcium sulfite. There is also a limit on chlorides, so the chlorides have to be controlled to a lower level in the absorber towers which can be an advantage to MOC life.

Most of the absorbers are designed with a 100% sized air blower (plus a 100% sized spare) that is sized for full load operation burning the design sulfur coal. The air blower may also be oversized to assure a large excess of oxygen to obtain the best quality gypsum possible. There are no provisions to vary the flow from the blower. This means that if a lower sulfur coal is burned or the unit is operated at lower load, there may be an extreme excess of oxygen present in the absorber slurry. Some ORP measurements taken in the latest generation of FGD systems have shown positive values more than double those seen in the older forced oxidation towers. There are discussions in the industry about the effect this highly oxidizing environment may be having on the absorber MOC.

Mixers

In the early days, mixers were fabricated by welding flat pieces of steel on a hub at an angle. This was done so the entire assembly could be rubber lined to withstand the abrasion of the slurry and the slurry chemistry. These mixers weren't that efficient, so one would normally find a mountain of solids in the center of the absorber tower. The floor under this mountain was subjected to under deposit corrosion.

With the new metals available, most of the newer mixers have a cast impeller shaped more like a propeller. These mixers move more fluid more efficiently. This increased flow has minimized the deposits settling to the floor.

Density

Originally the slurry density circulating in the absorber tower was in the 8 - 12% solids range. This was chosen to provide adequate reagent concentrations without requiring undue horsepower for the slurry recirculation pumps.

As operators began trying to grow saleable gypsum crystals or crystals that dewatered easily at the backend of the process, it was discovered that increased residence time and crystal concentration led to better crystal growth. Modern FGD systems operate with slurry density in the 15-20% solids range.

This increase in slurry density and crystal size has resulted in slurry droplets that are much more abrasive if they impact directly on a tower wall, slurry spray header or structural support.

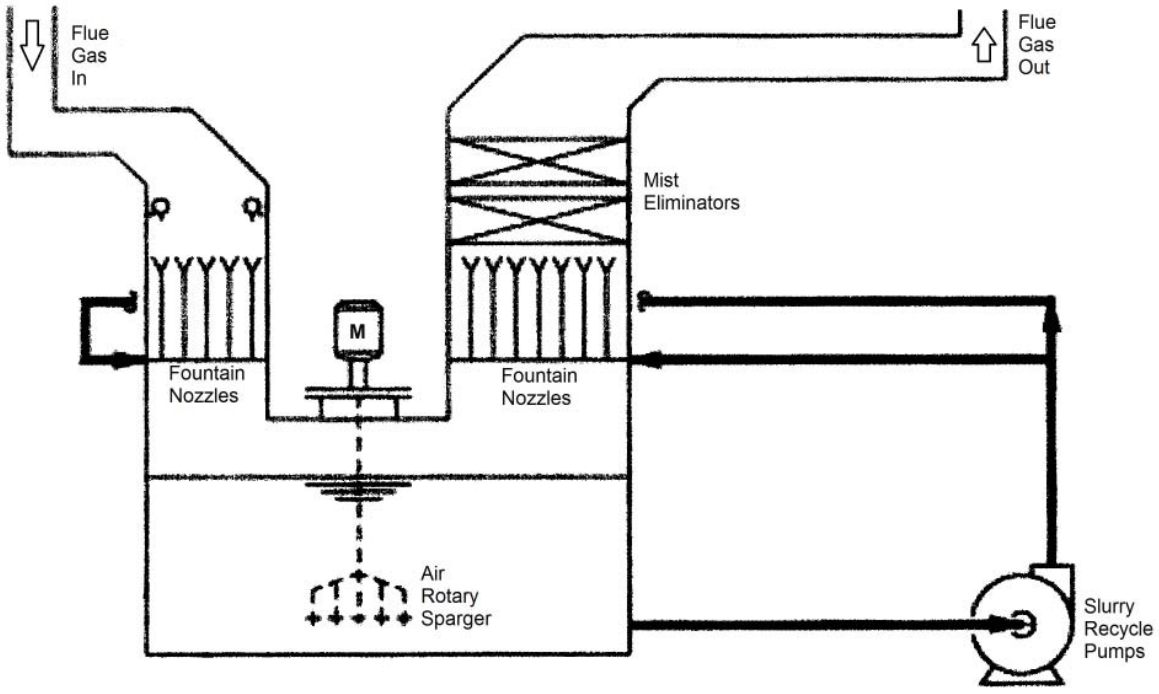

Figure 3. Fountain Nozzle Absorber Tower

Organic Acids

Once the regulatory requirement was for more than 95% removal of SO_2 from the flue gas, many operators using limestone as their reagent found this difficult. L/G ratios in the 120 - 150 range were being used. Research done in the past had proven that certain organic acids, when added to the absorber tower, made the limestone more effective in removing SO_2. The acids used are adipic, glutaric and succinic. These can decompose to valeric acid.

The concentrations of these acids is very small, so they should not have an affect on MOC. One may notice them in analytical work that might be done on the absorber slurry.

Waste Water Treatment

The latest environmental regulations are causing FGD system operators to treat any liquid streams that are leaving the system and entering bodies of water. They must address pH, metals, and other ionic species that would be harmful to the receiving body of water.

The cost of this can vary greatly depending on the volume of flow and how many treatment steps are required to address all of the items of concern. The cost can range from expensive to very expensive. This has put pressure on the designers and operators to tighten the system water balance to minimize the amount of liquid bleed that must be treated.

As mentioned earlier, when the water balance is tightened, the concentration of soluble ions such as chloride and fluoride increases in the system. If one is selling gypsum to wallboard manufacturers, there is a limit on how much chloride can be in the gypsum. So one is faced with keeping the chlorides under control in the entire system or letting them go to a higher level if one can effectively wash the chloride out of the gypsum on the vacuum filter.

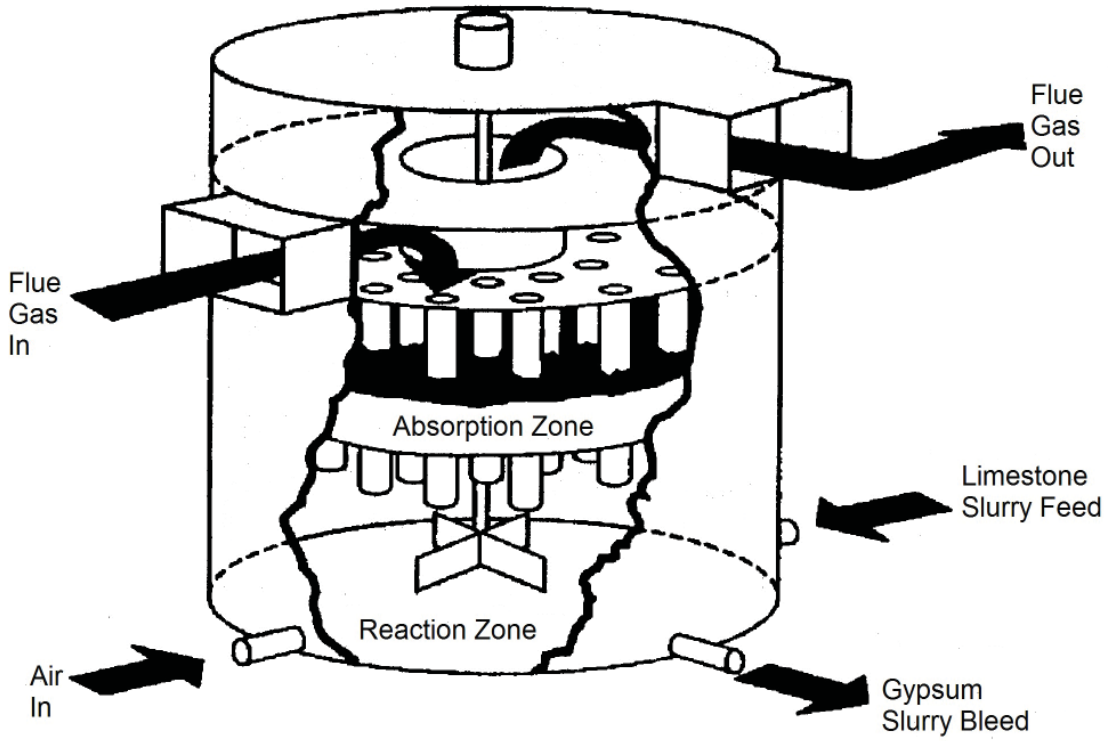

Figure 4. Jet Bubbling Reactor

People are handling this dilemma in different ways. One just needs to keep in mind that there is now a large economic incentive for being able to run with higher chlorides and fluorides in the FGD system rather than bleeding them out in a waste stream.

Fountain Nozzle Absorber Tower Design

One of the newer tower designs is the fountain nozzle tower. (see Figure 3) It is typically rectangular and not as tall as a spray tower. It is really a version of a spray tower rely-

ing on slurry droplets reacting with the flue gas to remove the SO_2. The difference is in how the droplets are formed. Instead of using high energy spray nozzles, individual solid streams of slurry travel vertically upwards from the slurry header. As gravity slows the liquid stream, the upward motion stops and the solid stream mushrooms out into a falling cascade of slurry droplets. This is similar to what one sees in a drinking fountain, hence the fountain nozzle name. After this happens, the slurry droplets and the flue gas interact just like they do in a spray tower.

The major difference for the MOC in this design is that there is minimal erosion occurring in the tower. The solid stream travels vertically up in an empty zone where it doesn't contact anything. The droplets form in an area of zero liquid velocity. Then the droplets fall under gravity. So there is little impact energy if the droplets contact anything. Most of these towers are limestone reagent with forced oxidation, so there is little scale formation in the absorber tower.

Jet Bubbling Reactor Design

The other newer tower design is the jet bubbling reactor (JBR). (see Figure 4) This design is completely opposite of the other tower designs. There are no pumps to recirculate the slurry. The slurry remains in the tower sump at all times. Large axial fans are used to generate the pressure needed to bubble the flue gas through hundreds of large "straws" that are submerged into the top of the slurry pool. The principal is exactly like blowing through a straw submerged in a beverage glass.

The flue gas bubbles out of the end of the straws. The hot gas/liquid interface is at the end of the straw submerged in the liquid pool. The SO_2 reaction with the alkali is on the surface of the gas bubbles. The rising bubbles also create a froth layer which gives more reaction surface area.

The tower is physically divided into three separate compartments.

- The center elevation is where the hot flue gas enters the tower. The floor of this compartment is penetrated by the tops of all the straws taking the flue gas into the lower compartment.

- The lower compartment is filled with slurry to an elevation that will cover the lower end of the straws to the desired depth. A layer of froth will form on top of the slurry and then there is free space for the cleaned flue gas to collect. Several large riser tubes will take the collected clean flue gas and route it through the center compartment and release it into the upper compartment.

- From the upper compartment, the gas travels into the outlet duct to the chimney. The mist eliminator is located in the outlet duct downstream of the JBR tower outlet.

The JBR operates in the forced oxidized mode. Air enters the slurry pool through a series of air spargers. JBR towers have been known to grow large gypsum crystals due to the flow conditions in the lower compartment. There are no strong slurry flows to create erosion and the forced oxidation minimizes scale formation.

There is typically some quenching of the hot flue gas using spray nozzles in the inlet duct before it enters the center compartment. There have been some scaling and corrosion issues at this location. There have also been reports of gypsum buildup on the floor of the JBR tower.

Most of the JBR fleet has entered service in the last few years, so there isn't the large body of long term experience to look at like there is for the spray towers.

RE Consulting

For further information contact Ron Richard at ron.richard@reconsulting.info

Ron Richard, a senior consultant for RE Consulting, is a chemical engineer who has specialized in Operations and Maintenance of FGD and SCR systems.

Ron's 32 years of utility experience with Cinergy included engineering, testing and maintenance of water treatment and lime handling systems, coal analysis procedures and practices for ASTM compliance, piping design and installation of bearing cooling water systems, design and construction of FGD and SCR systems, as well as procurement of catalysts for NOx removal. Ron has been member of various Electric Power Research Institute (EPRI) committees and advisory groups and has published numerous articles on the FGD and NOx topics.

Description of a Pseudo-Particulate Formation Mechanism in New EPA Method 202

By: Jack Bionda, Clean Air Engineering

Introduction

The recent modifications promulgated by EPA to the Method 202 sampling system were thought to resolve most if not all of the significant limitations of "old" Method 202. These modifications, shown in Figure 5, include the re-design of the sampling system to include a glass-coil (modified Graham) condenser, two dry impingers, and an unheated condensable particulate matter (CPM) filter. The modifications were implemented in order to eliminate the significant CPM "artifacts" which often occurred in old Method 202.

In new Method 202, the CPM is collected in dry impingers after filterable particulate matter (FPM) has been collected on a filter maintained as specified in either Method 5, 17, or 201A. New Method 202 eliminates the use of water as the collection media in impingers and includes the addition of a condenser followed by a water dropout impinger immediately after the final in-stack or heated filter.

This article presents the results of a recently completely test program conducted on a coal-fired boiler using new Method 202, and discusses the potential for pseudo-CPM formation in the new method.

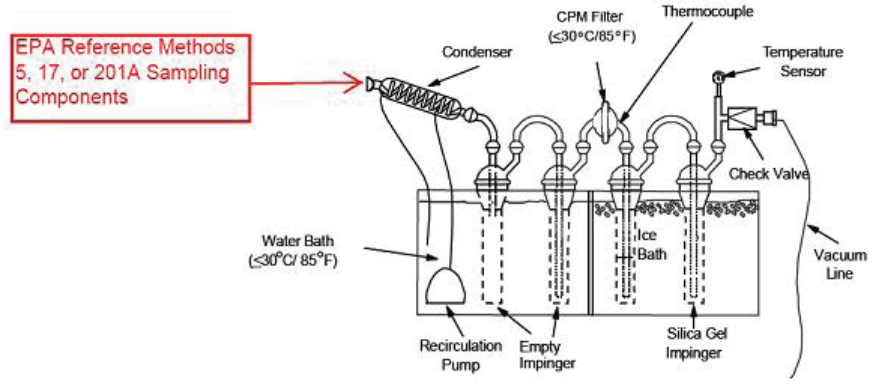

Figure 5.
EPA Method 202 (New) Sampling System

Background on Old Method 202

Source emission testing experience since the promulgation of Method 202 in 1991 demonstrated that it was inappropriate to use water-filled impingers to cool the sample gas stream for CPM combustion sources having SO_2, NO_2 and/or soluble organic compound emissions. These gaseous contaminants can partially absorb in the impingers and chemically oxidize to form material counted as CPM in old Method 202. These artifact reaction products are not related to the primary emission of CPM from the source.

The potentially significant problems affecting the accuracy of old Method 202 included the following:

1. Dissolution of sulfur dioxide and nitrogen oxides into water with subsequent oxidation to form sulfates and nitrates in the impingers;
2. Dissolution of soluble organic compounds into water;
3. Penetration of submicrometer sized condensed particles through the impingers of the Method 202 sampling train;
4. Gas phase homogeneous reactions between ammonia and hydrogen chloride and/or between ammonia and sulfur dioxide in the cold, water-filled impingers.

Of these four sources of bias, the absorption and reaction of sulfur dioxide was most common. Since old Method 202 was originally promulgated, there was considerable concern that absorption of soluble sulfur dioxide and nitrogen dioxide and subsequent reactions of these dissolved gases occur within the aqueous phase in the impingers. These reactions

are important because these gases are considerably more soluble in cold liquids than in warm liquids. The 32°F to 68°F temperatures of the liquid in the impingers provide an ideal environment for the collection of soluble inorganic gases.

Description of the Unit Tested

For the purposes of this discussion, the boiler tested will be identified as Unit A. Unit A is a solid fuel-fired steam generating unit that utilizes circulating fluidized bed (CFB) boiler technology to burn low sulfur Powder River Basin (PRB) coals. Unit A has a nameplate rating of approximately 400 MMBtu/hr. The boiler was designed for a maximum continuous rating of 300,000 lb/hr of steam flow at a pressure of 150 psig, and temperature of 450°F. Unit A is equipped with an in-bed limestone sorbent injection system for the control of SO_2 emissions and to protect internal waterwall surfaces from sulfide corrosion. Nitrogen oxides (NOx) are controlled by the low inherent combustion temperatures with staged combustion. Additional NOx control is provided by a selective non-catalytic reduction (SNCR) system, which injects ammonia (NH_3) into the appropriate high temperature region of the furnace for conversion of NOx to N_2 and H_2O. Figure 6 shows a process diagram of Unit A.

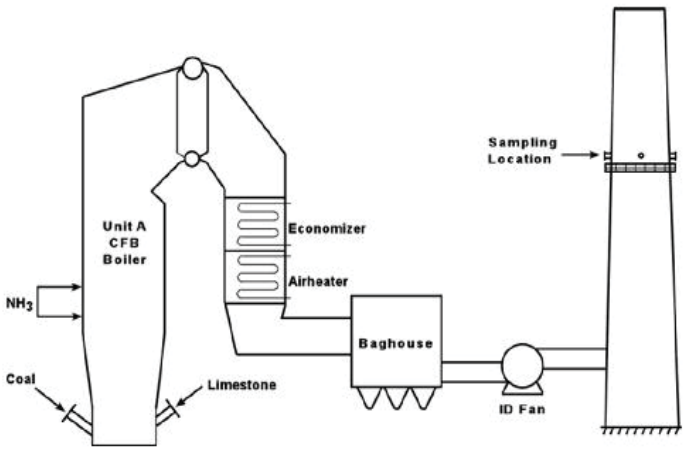

Figure 6. Process Diagram of Unit A

Description of Testing

CleanAir conducted compliance testing of Unit A in 2010. The compliance testing consisted of three (3) runs of EPA Method 5/202 for the determination of FPM/CPM, as well as simultaneous controlled condensation method (CCM) testing using CleanAir Method 8B (modified EPA CTM-013) for the determination of H_2SO_4. Unit A has operating permit limits for FPM, CPM, and H_2SO_4. All testing was conducted at the stack.

During the 2010 compliance testing of the Unit A, elevated condensable particulate matter (CPM) were detected in the back-half fraction of the EPA Method 5/202 sampling system. Utilizing ion chromatography (IC) analysis of the back-half fractions, it was determined that approximately 85% of the inorganic CPM consisted of ammonium sulfate compounds. These compounds were determined to be "artifacts" and should not be considered measured condensable material. This paper explains the formation mechanism for ammonium sulfate which is believed to have occurred in the Method 202 sampling system.

Discussion of the Pseudo CPM Formation Mechanism

The formation of the pseudo-particulate ammonium sulfate compounds which were found in the Method 202 "dry" impingers during the 2010 compliance testing of the Unit A boiler are the result of chemical reaction of dissolved sulfur dioxide (SO_2) and ammonia (NH_3).

This pseudo-particulate is the result of the dissolution (i.e. scrubbing) and subsequent reaction of flue gas SO_2 and ammonia NH_3 slip from the Unit A boiler selective non-catalytic reduction (SNCR) system which forms either ammonium bisulfate or ammonium sulfate according to the following reactions:

$$NH_3\ (gas) + SO_2\ (gas) + H_2O \rightarrow NH_4\ (liq) + HSO_3\ (liq) + time,\ O_2 \leftrightarrow (NH_4)HSO_4 \quad (1)$$

$$2NH_3\ (gas) + SO_2\ (gas) + H_2O\ (liq) \rightarrow NH_4\ (liq) + SO_3\ (liq) + time,\ O_2 \leftrightarrow (NH_4)_2SO_4 \quad (2)$$

Sulfur dioxide itself is a gas that readily dissolves in water. Once dissolved, it reacts with water to form new compounds called *sulfites*, according to the following reaction:

$$H_2O + SO_2 \leftrightarrow H+ + HSO_3^- \leftrightarrow 2H+ + SO_3^= \quad (3)$$

In solution with H_2O (water), SO_2 is called molecular SO_2, HSO_3^- is called bisulfite and $SO_3^=$ is called sulfite. The negative signs ($^-$ and $^=$) denote the negative charge of the bisulfite and sulfite ions (molecules with a charge are called ions). The double arrows (↔) of the equation denote that the reaction is at equilibrium.

Solubility of Ammonia and Sulfur Dioxide in Water

Many gases are soluble in water, particularly NH_3 and SO_2. The solubility of SO_2 and NH_3 in water are shown in

Figures 7 and 8, respectively.

New Method 202 requires that the dry impingers are operated at a temperature less than 85°F (29°C). In practicality, these impingers are typically operated in the temperature range of 60°F to 84°F (16°C to 29°C). This temperature range is below the dew point temperature of the flue gas. All gases have a dew point that is dependent on the temperature, pressure, fuel type and sulfur content. Below the dew point temperature, the gas/vapor will start to condense into liquid. The dew point temperature of a flue gas having a water vapor content of 17% vol. H_2O, such as the stack gas of the Unit A boiler, would be approximately 128°F (53°C).

Ammonia gas has a high affinity for water. As seen in Figure 8, its solubility in water at 68°F (20°C) is approximately 520 mg/g. The solubility of sulfur dioxide in water at 68°F (20°C) is approximately 120 mg/g. The presence of ammo-

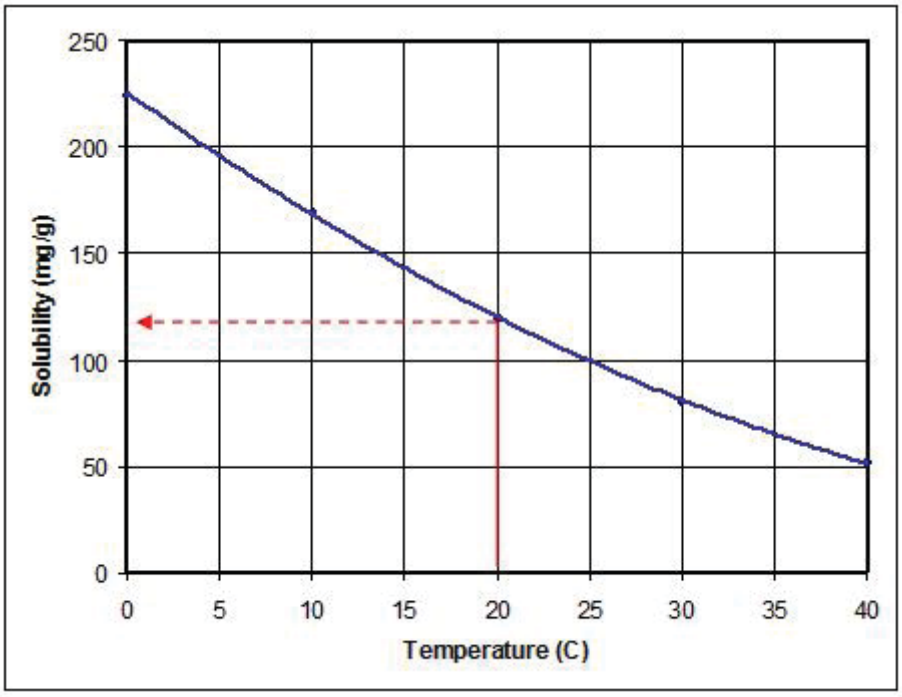

Figure 7.
Solubility of SO_2 in Water

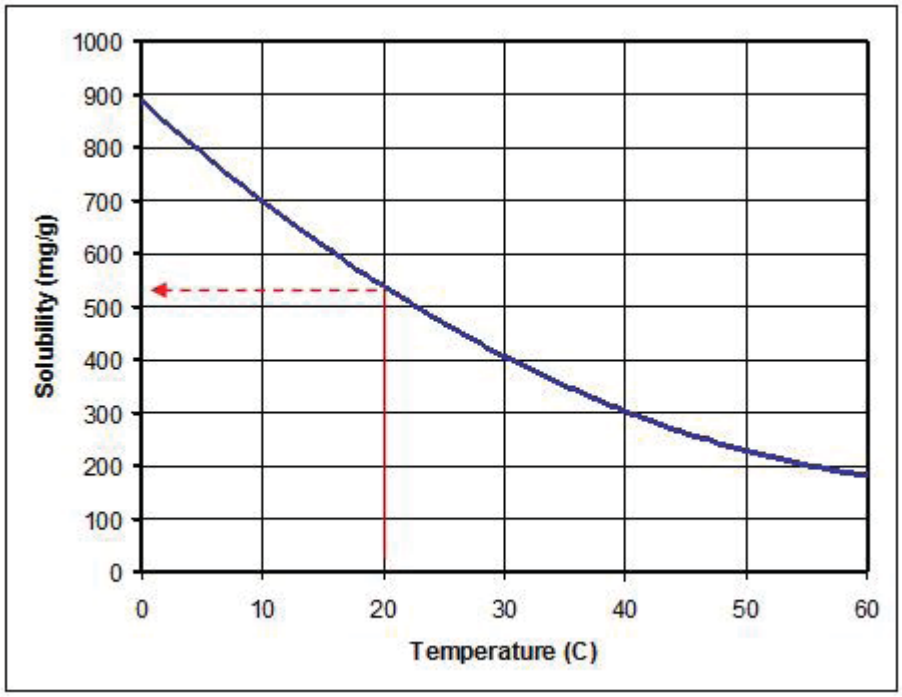

Figure 8.
Solubility of NH_3 in Water

nia in the gas stream enhances the solubility (absorption) of SO_2 – in the condensate. So much so that bubbling the gas through the liquid does not have to occur.

Ammonia, being extremely water soluble, will first absorb into the condensate elevating the pH. This slight elevation in pH will greatly enhance artifact generation through scrubbing of sulfur dioxide, forming various dissolved ammonium sulfate salts.

The excess ammonia is the chemical driving force, greatly increasing the solubility of SO_2. This is occurring in a thin film, without bubbling through the solution. This is due to ammonia's affinity for water, forming a basic solution that wants to attract and react with the acidic SO_2 gas.

Analytical Determination of Ammonium Sulfate and Correction of Inorganic Results

The post-test analysis of the inorganic CPM fraction of the Method 202 samples consisted of taking a 20-ml aliquot of the dry impinger liquid and associated rinse prior to the gravimetric analysis which includes the extraction and evaporation steps. This aliquot was analyzed for both anions and cations using Dionex ion chromatography (IC) in CleanAir's analytical laboratory. The only anions and cations identified by IC were sulfate ($SO_4^{=}$) and ammonium (NH_4^{+}), respectively.

Using the results from the IC analysis, it was determined that Run 1 had a stoichiometric excess of ammonium, and Runs 2-3 had an excess of sulfate. Equation 4 below was used to make this determination:

$$\text{mg } SO_4^{=} \times \frac{1 \text{ mol } SO_4}{96.0 \text{ mg } SO_4} \times \frac{2 \text{ mol } NH_4}{1 \text{ mol } SO_4} \times \frac{18 \text{ mg } NH_4}{1 \text{ mol } NH_4} = \text{mg } NH_4 \text{ required} \qquad (4)$$

As a simplification that expresses the most conservative results, we assumed that ammonium sulfate was formed preferentially in all three Runs. This assumption seemed reasonable given the concentrations of the reactants, and the pressure and temperature of the impinger. The chemical reaction equation for the formation of ammonium sulfate is as follows:

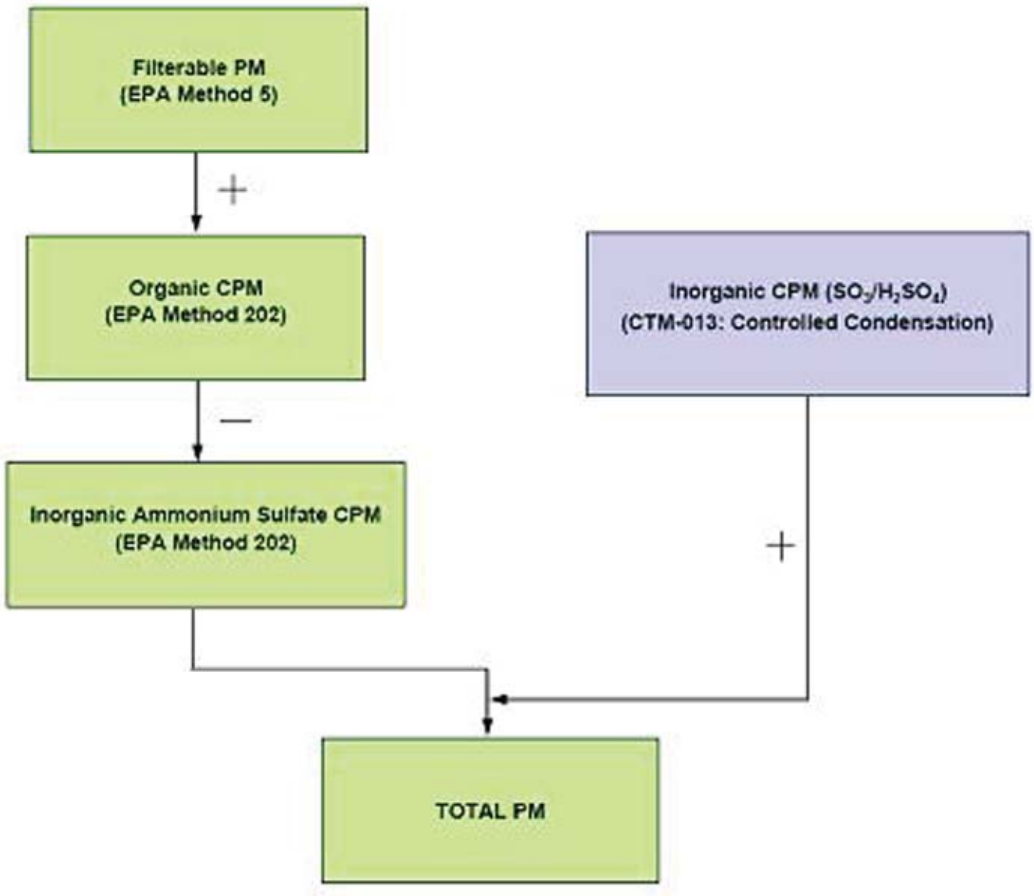

Figure 9. Total Particulate Matter Determination Flow Chart

$$H_2SO_4 + 2NH_3 \rightarrow (NH_4)_2SO_4 \qquad (5)$$

Therefore, the stoichiometric mass of ammonium sulfate formed using the ammonium IC data, was determined using the following expression:

$$\text{mmol } NH_4 \times \frac{132.14 \text{ g}}{\text{mol}} \times \frac{1 \text{ mol } (NH_4)_2SO_4}{2 \text{ mol } NH_4} = \text{mg } (NH_4)_2SO_4 \qquad (6)$$

Concurrent to the Method 5/202 particulate testing, controlled condensation method (CCM) measurements were performed in the Unit A stack in order to quantify the sulfuric acid (H_2SO_4) emissions. Sulfuric acid emissions are a "real" inorganic CPM, and are considered a $PM_{2.5}$ precursor. The CCM samples were also analyzed using IC by CleanAir.

The inorganic CPM gravimetric results were then corrected based upon the above results, using the expression shown in Equation 7:

Inorganic CPM, corrected =

Aliquot Corrected Sample Net ($M_{n,Corr}$) – Stoichimetric Mass of Ammonium Sulfate [$(NH_4)_2SO_4$] + Volume Corrected Stoichiometric Mass of Sulfuric Acid ($H_2SO_{4,corr}$) **(7)**

Figure 9 (shown on page 12) shows the flow chart of the procedures used to determine the corrected total particulate matter results.

Discussion of Results

Figures 10, 11 and 12 (shown on page 14-15) show the particulate testing results for the three compliance runs. In order to protect anonymity of the client, the data has been normalized by assigning a dimensionless value of 1 to the uncorrected total particulate matter ($TPM_{,unc}$) results for each test. The filterable particulate matter (FPM), uncorrected condensable particulate matter ($CPM_{,unc}$), corrected condensable particulate matter ($CPM_{,cor}$), sulfuric acid CPM (H_2SO_4 CPM), corrected total particulate matter ($TPM_{,cor}$), and ammonium sulfate (pseudo CPM) are expressed as a fraction of the uncorrected total particulate matter results.

The magnitude of the ammonium sulfate artifact is easy to distinguish in these charts. The ammonium sulfate pseudo CPM averaged approximately 85% of the uncorrected total particulate matter for the three runs. The unit TPM permit limit is shown as a dashed red line. As is apparent in these figures, the dissolution of the NH_3 in the dry impingers, and its subsequent reaction with SO_2 to form ammonium sulfate is the sole reason Unit A exceeded its permit limit during the compliance testing performed in 2010. When the pseudo CPM is accounted for, Unit A is significantly under its permit limit for TPM.

EPA's Position

The new version of EPA Method 202 contains a new definition of CPM. Section 3.1 of new Method 202 states:

> *"CPM means material that is vapor phase at stack conditions, but condenses and/or reacts upon cooling and dilution in the ambient air to form solid or liquid PM immediately after discharge from the stack."*

In old Method 202, CPM was defined in terms of the test method as follows:

> *"This method applies to the determination of condensable particulate matter (CPM) emissions from stationary sources. It is intended to represent condensable matter as material that condenses after passing through a filter and as measured by this method".*

In other words, "condensable" in old Method 202 meant condensable in the impinger. Condensable in the new method means particulate that forms as the result of either condensation or reaction in ambient air. This new definition represents something of a sea change in the way condensable particulate matter is defined, because it leaves open the question of what is actually occurring in the ambient air at or very near the stack exit, which cannot be directly quantified with this method.

Therefore, what constitutes CPM is left open to some extent to the discretion of EPA. That is to say that by broadening the definition of CPM to include atmospheric chemical reactions, EPA has essentially defined away the entire concept of measurement artifacts in Method 202. EPA has stated that they believe that NH_3 and SO_2 will react preferentially in the ambient air to form ammonium sulfate or related compounds. They have provided very limited evidence to support this position.

Sulfate Formation in Laboratory Clouds

Hansen et al. examined SO_2 oxidation in the presence of NH_3 in a mixing-type continuous-flow cloud chamber. The tests

performed by Hansen were intended to simulate combustion-produced SO_2 discharged into a fog cloud.

In the Hansen apparatus shown in Figure 13 (page 16), a warm, humidified, particle-laden air stream is introduced axially through the bottom plate of the cylindrical glass chamber of 16 cm inside diameter, 150 cm height. It mixes with an annular flow of cold, dry dilution air to produce the cloud by cooling the mixture below the resultant dew point.

Sodium chloride (NaCl) and propane soot particles (~ 5-15 µg/m^3) were used as cloud condensation nuclei. Cloud liquid water content was varied between 0.2 and 3 g/m^3. SO_2 and NH_3 concentrations were 0.6 and 1.1 ppm, respectively. The contact time between the SO_2 and the cloud drops was varied from 8 s to 3 min. Up to 80% of the input SO_2 can be oxidized to sulfate within short contact times in the presence of NH_3 and when the water is in the condensed cloud-drop phase. Negligible sulfate formation was observed in the absence of the liquid phase regardless of the presence or absence of NH_3. No significant dependence of the oxidation on the cloud condensation nuclei type nor the contact time was found.

Conclusions

The following conclusions have been made based upon the test results and research conducted on this issue:

- The reactions in equations 1 and 2 are dependent on dissolution of SO_2 and NH_3 in water and the temperature of the impingers; they would not normally take place anywhere in or beyond the stack exit. A nitrogen purge will have no effect in removing the ammonia salts once formed. The only way to account for these pseudo-particulates is to quantify the ammonium salts in the impinger catch using ion chromatography or selective ion electrodes, and account for them using a stoichiometric mass balance.

- The excess ammonia is the chemical driving force, greatly increasing the solubility of SO_2. This is occurring in a thin film, without bubbling through the solution. Because of ammonia's affinity for water, a basic solution is formed in the impingers that attracts and reacts with the acidic SO_2 gas forming ammonium salts.

- The particulates found in the impinger are not found in the stack since the two reacting compounds must be in gaseous form to pass through the initial (EPA Method 5) particulate filter.

- The ammonium salts are not formed by condensa-

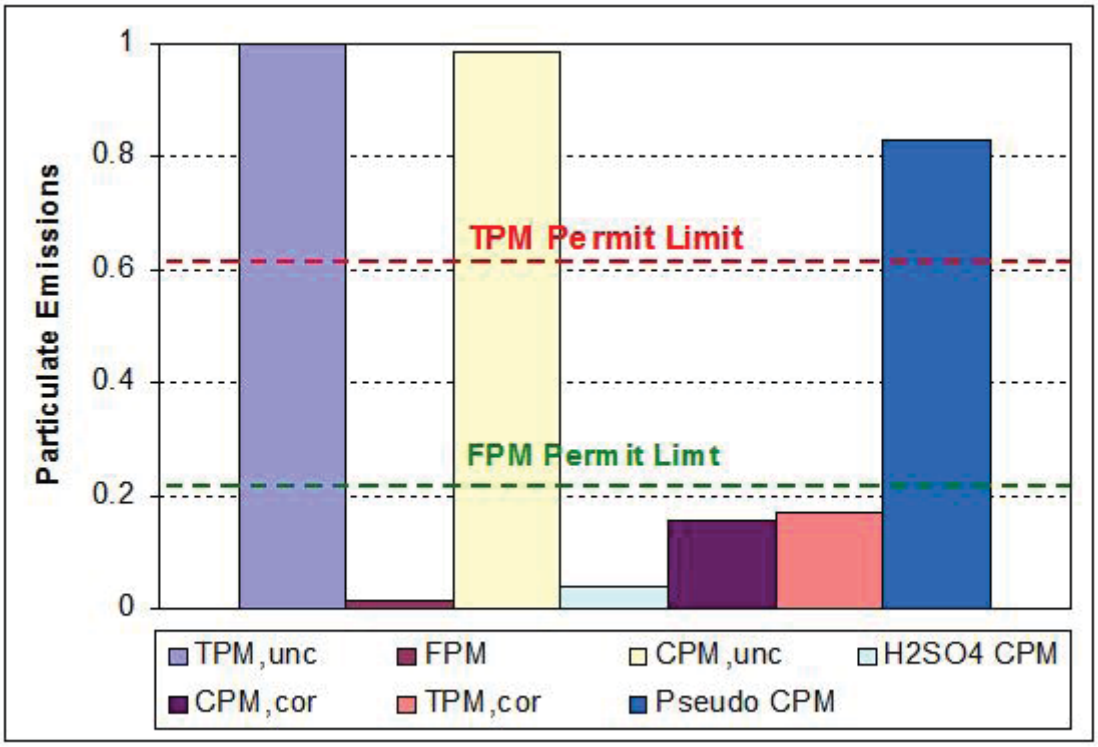

Figure 10. Run 1 Results Summary

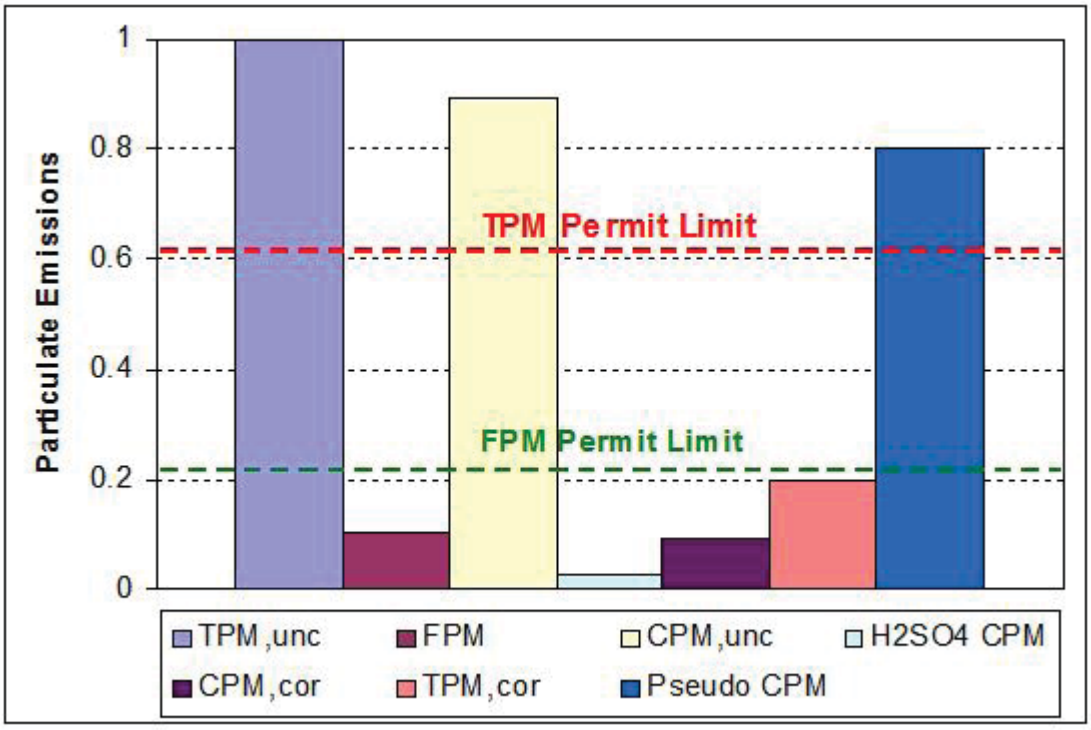

Figure 11. Run 2 Results Summary

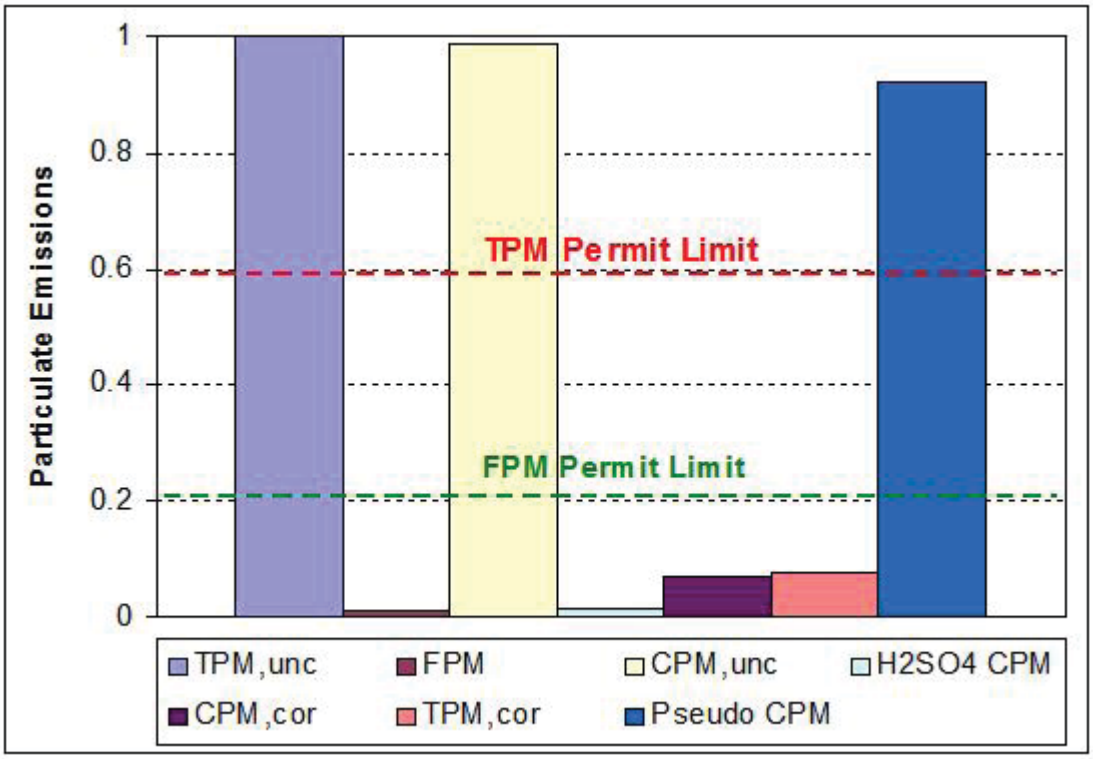

Figure 12. Run 3 Results Summary

tion, but rather require a reaction between dissolved SO_2 and NH_3, in the presence of water.

- The artifact CPM formation mechanism described in this document is likely to occur in any source that has appreciable levels of free ammonia in the flue gas, coincident with low sulfuric acid concentrations.
- Cloud chamber research by Hansen showed that SO_2 and NH_3 will not react in the absence of liquid water droplets.
- Work of Hansen indicates that SO_2 and NH_3 would not react immediately at the exit of a stack to form CPM.
- The EPA should acknowledge that significant positive biases related to the interaction of SO_2-NH_3-H_2O can occur in new Method 202, and should allow for quantification and correction of these biases using procedures similar to those outlined in this article.

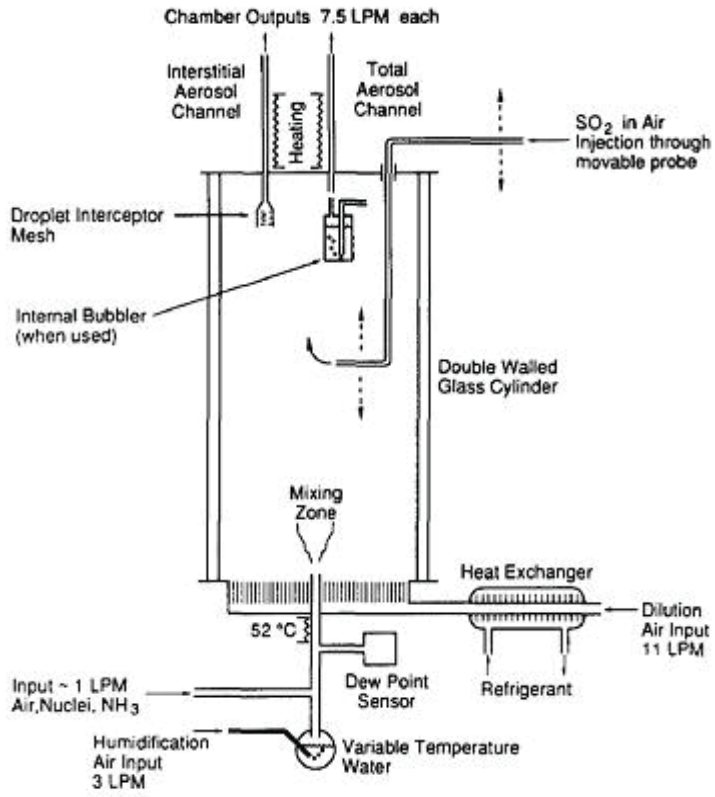

Figure 13. Schematic Diagram of Hansen Cloud Chamber Apparatus

CleanAir®

For further information contact Jack Bionda at jbionda@cleanair.com

Jack Bionda is a Principal Engineer in Clean Air Engineering's Consulting Services Group. He has over 20 years of experience in the fields of combustion engineering, diagnostic boiler testing, boiler operations and consulting.

Prior to joining Clean Air Engineering, he worked as a project engineer for Energy Systems Associates. He has participated in the development of energy/environmental solutions from pilot-scale to commercialization stage. He has managed and led applied research projects analyzing impacts of flue gas treatment systems on ancillary equipment such as electrostatic precipitators. He's also participated in the development and promulgation of new environmental emission test standards. Mr. Bionda earned a B.S. degree in Mechanical Engineering from Pennsylvania State University.

Welcome to WPCA's Newest Corporate Sponsors

Mississippi Lime

Norit-Americas

and the new WPCA Officers

- **Melanie McCoy**
- **Doug Hartman**
- **Cindy Khalaf**
- **Rob Mudry**
- **Paul Ford**

Larger Multiple-Tube Mechanical Dust Collectors Are Not Always Better

By Chris McKeown, Babcock & Wilcox

Multiple tube mechanical dust collectors have been used since the early 20th century for collecting particulate within a gaseous process. They have been used for many different applications such as emission control devices, product collection and equipment protection. The efficiency of a multiple tube mechanical dust collector depends on many factors such as particulate size, particle distribution, process pressure / temperature, gas properties and others. One of the main factors that contribute to the collection efficiency of the multiple tube mechanical dust collector is the size of the collecting tube itself. When it comes to selecting a multiple tube mechanical dust collector, bigger is not always better, if collection efficiency is taken into consideration.

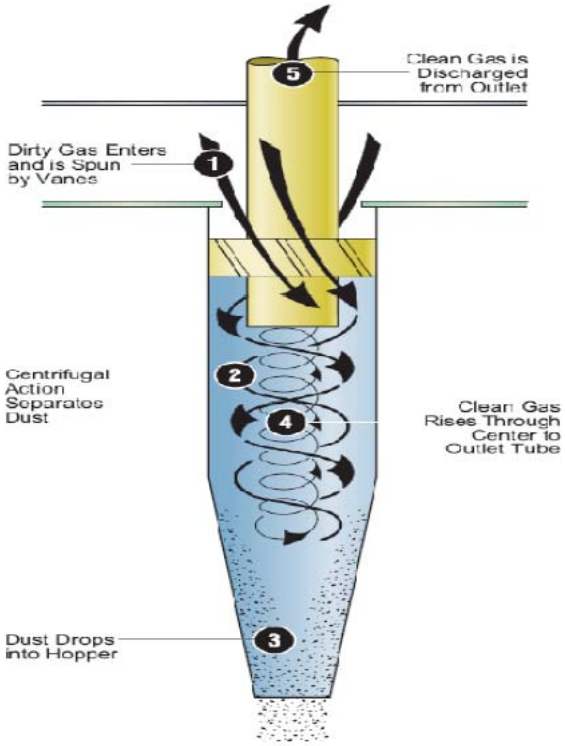

Figure 14. Illustrates How the Centrifugal Force is Used to Separate the Particles From the Gas Stream.

According to Sir Isaac Newton, a mechanical dust collector with a larger diameter is not better at collecting particulate. In fact, Newton's "Laws of Motion" clearly state "every object will remain at rest or in uniform motion in a straight line unless compelled to change its state by the action of an external force." In this case the object is a particle within a dirty gas stream. If all the external forces cancelled each other out, the velocity would remain constant or remain still if the velocity was equal to zero. The particles within the collection area of a mechanical dust collector are subject to many external forces. Some of the forces include gravity, pressure, centrifugal force and friction caused by gas viscosity. The velocity of a particle is changed when the net force of all external forces do not cancel out and are exerted onto the particle.

According to Newton's 2nd law, the force that creates the change in velocity is equal to the mass of the particle, times the acceleration ($F= m \cdot a$). When discussing particles that are spun through a vane in the collecting tube, the formula can be substituted as $F=m \bullet ac$, where ac is equal to the centripetal acceleration. This is calculated by squaring the velocity (m/sec) and then dividing the result by the radius of the collecting tube ($ac = v^2/r$). By substitution centripetal force (Fc) is equal to $Fc= m \cdot v^2/r$.

Once the centrifugal force is determined, it can be used along with gravitational force, coefficient of friction, drag coefficient and force, buoyant force and other external forces to determine the particle settling velocity. The settling velocity is the speed in which a particle falls out after overcoming the force of gravity and the force of drag. For simplicity and keeping to the point of collecting tube diameter vs. collection efficiency, centrifugal force will be used to explain how smaller is better, assuming all other factors are equal. Figure 14 illustrates how the centrifugal force is used to separate the particles from the gas stream.

For example, suppose a footprint area of 16 x 16 feet is used to design a multiple tube mechanical dust collector. A 24-inch collecting tube unit can fit 49 tubes. A 12-inch tube unit can fit 144 tubes and a 9-inch tube unit can fit up to a 256 tubes. Unfortunately, it is not that simple. If the footprint area is filled with the maximum number of tubes that can fit into it, other design factors, such as differential pressure, maximum tube velocity and maximum actual cubic feet per minute (ACFM) per tube, change and an equal comparison cannot be made. If the mentioned tube quantities are used with an ACFM of 135,000, a process temperature of 500°F and a particle mass of 5kg, the following results are gen

24inch Collecting Tubes			12inch Collecting Tubes			9inch Collecting Tubes		
Tubes	dP		Tubes	dP		Tubes	dP	
49	1.95		144	1.58		256	4.20	
M (Mass)	5	kg	M (Mass)	5	kg	M (Mass)	5	kg
V (Gas Velocity)	18.37	m/sec	V (Gas Velocity)	13.83	m/sec	V (Gas Velocity)	26.11	m/sec
r (tube radius)	0.36	m	r (tube radius)	0.18	m	r (tube radius)	0.135	m
Centrifugal Force =	4,685.5	N	Centrifugal Force =	5,311.1	N	Centrifugal Force =	25,241.8	N

Figure 15

erated for centrifugal force. Notice the difference with the differential pressure, when the design footprint is filled completely with tubes.

Since differential pressure is equal to the amount of energy put into the system, we will adjust the amount of tubes so that all three size units have close to the same pressure loss.

24inch Collecting Tubes			12inch Collecting Tubes			9inch Collecting Tubes		
Tubes	dP		Tubes	dP		Tubes	dP	
32	4.39		88	4.22		256	4.20	
M (Mass)	5	kg	M (Mass)	5	kg	M (Mass)	5	kg
V (Gas Velocity)	28.13	m/sec	V (Gas Velocity)	22.63	m/sec	V (Gas Velocity)	26.11	m/sec
r (tube radius)	0.36	m	r (tube radius)	0.18	m	r (tube radius)	0.135	m
Centrifugal Force =	10,986.3	N	Centrifugal Force =	14,221.3	N	Centrifugal Force =	25,241.8	N

Figure 16

By reducing the amount of tubes to fit the same footprint and have the same pressure drop, the results in Figure 16 show that the 9-inch unit has the highest amount of force. The 9-inch unit is more than double the amount of the 24-inch unit. The 12-inch unit has less force than the 9-inch but much higher force than the 24-inch tube unit.

In conclusion, the above results, which are based on Sir Isaac Newton's Laws of Motion, prove that the centrifugal force that is produced within a collecting tube is less in larger diameter tubes. Since centrifugal force is the energy that separates the particles from the gas, it is conclusive to say that BIGGER is NOT BETTER. With all things being equal in the example shown, the radius of the collecting tube is indirectly proportional to the force produced to clean the dirty gas. As the radius of the collecting tube decreases, the centrifugal force increases.

For further information contact Chris McKeown at cjmckeown@babcock.com

Chris McKeown is the Product Manager for B&W's Environmental Aftermarket Western Precipitator product line. He has over 20 years experience as a Technical Service Representative in various industries including Catalyst Systems, Fuel Cells, Polymer Science and Textiles. He has recently taken on the role as a Product Manager for B&W's Multiclone® Mechanical Dust Collector, Wet ESP and Turbulaire™ Scrubber product lines. When Chris is not working on business development opportunities, in the office, he spends his time in the field assisting customers with unique particulate control applications. Chris has a B.S. in Business Management and an Associate's Degree in Science & Engineering Technologies.

A Mechanistic Study on the Inhibition of the DENOX Reaction on the Mercury Oxidation Over SCR Catalysts

By Karin Madsen, Haldor Topsoe A/S; Anker D. Jensen, Technical Institute of Denmark; Flemming J. Frandsen, Technical Institute of Denmark; Joakim R. Thogersen, Haldor Topsoe A/S

Abstract

The vanadium-based SCR catalyst used for NOx control promotes the oxidation of elemental mercury Hg^0 to Hg^{2+} in flue gases from coal-fired power plants. Hg^{2+} is water soluble and can effectively be captured in a wet scrubber. This means that the combination of an SCR with a wet FGD can offer an effective control option for mercury.

Laboratory experiments have been carried out to elucidate and quantify the inhibition by the DeNOx reaction on the Hg^0 oxidation by HCl over commercial SCR catalysts under different operating conditions. In the presence of NO and NH_3, the following three net reactions have been identified as relevant for the mercury chemistry over the SCR:

$$\mathbf{R1:\ 2\ HCl + Hg^0 + \tfrac{1}{2}\ O_2 \leftrightarrow HgCl_2 + H_2O}$$

$$\mathbf{R2:\ 2\ NH_3 + 3\ HgCl_2 \leftrightarrow N_2 + 3\ Hg^0 + 6\ HCl}$$

$$\mathbf{R3:\ 2\ NO + 2\ NH_3 + \tfrac{1}{2}\ O_2 \leftrightarrow 2\ N_2 + 3\ H_2O}$$

Reaction R1 is the oxidation of Hg^0 with HCl, reaction R2 is the reduction of $HgCl_2$ with NH_3 and reaction R3 is the DeNOx reaction.

The importance of the different reactions on the Hg^0 oxidation depends on the SCR operating temperature. At T>325ºC, reduction of $HgCl_2$ with NH_3 will take place. The observed Hg^0 oxidation will reflect the relative rate of the Hg^0 oxidation via reaction R1 and the $HgCl_2$ reduction via reaction R2. For T=250-375ºC, the DeNOx reaction will inhibit the kinetics of reaction R1 by consuming active Lewis sites that must be oxidized to regain activity for Hg^0 oxidation.

Experimental data obtained in this study indicate that vanadia Lewis sites on the catalysts are active in the catalytic Hg^0 oxidation – possibly as Hg^0 adsorption sites.

Introduction

The oxidation of Hg^0 over full-scale SCR reactors has been reported in the range of 4-98% depending on coal rank/type, operating conditions and catalyst type/geometry. The sources to the considerable scatter in the level of Hg^0 oxidation in full-scale remains poorly understood. In the quest of optimizing the Hg^0 oxidation for different SCR applications, a greater fundamental understanding of the relevant mercury chemistry over the SCR catalysts is needed.

Chlorine is primarily responsible for the oxidation of Hg^0 via the following net reaction:

$$\mathbf{2\ HCl + Hg^0 + \tfrac{1}{2}\ O_2 \leftrightarrow HgCl_2 + H_2O}$$

The concentration of chlorine in the coal has repeatedly been identified to be a major determining factor for the observed Hg^0 oxidation over different SCR applications, where an increasing oxidation is seen for increasing chlorine.

The concomitant NOx-reduction by NH_3 (DeNOx-reaction) over the SCR inhibits the Hg^0 oxidation by HCl. Laboratory experiments have shown the following two effects on the mercury chemistry from the DeNOx-reaction:

1. The Hg^0 adsorption on SCR catalysts decreases in the presence of the DeNOx reaction,

2. The presence of NH_3 in the flue gas can result in a reduction of $HgCl_2$ to Hg^0 over the SCR.

The first effect may cause a decrease in the rate of Hg^0 oxidation over the SCR by inhibiting the initial step in the catalytic reaction. The second effect suggests that a reducing reaction is taking place concurrently to the Hg^0 oxidation thus lowering the overall oxidation of Hg^0 achieved over the SCR. If it is by one of these mechanisms (or by a completely different effect) that the presence of the DeNOx is influencing the overall Hg^0 oxidation remains unclear.

This study serves to elucidate and quantify the effect of the DeNOx reaction on the Hg^0 oxidation by HCl over commercial SCR catalysts under different operating conditions.

Experimental

Catalyst: Commercial corrugated-type monoliths obtained from Haldor Topsøe A/S are applied in this study. The catalysts are based on V_2O_5 and WO_3 dispersed on a fibre reinforced TiO_2 carrier. The geometry and the dimensions of the

tested catalysts are identical in all the experiments, so data is directly comparable.

Laboratory Setup: The mercury chemistry over SCR catalysts is studied in a laboratory setup at Haldor Topsøe A/S. Here a simulated flue gas containing Hg^0 or $HgCl_2$ is passed through a SCR reactor and the change in mercury speciation is measured for different operating conditions, gas compositions and catalyst compositions. A schematic drawing of the setup is given in Figure 17. The setup consists of a mixing module, where all gases are mixed and preheated, a SCR reactor, a reduction unit (to reduce all $HgCl_2$ to Hg^0) and a mercury (Hg^0) analyser.

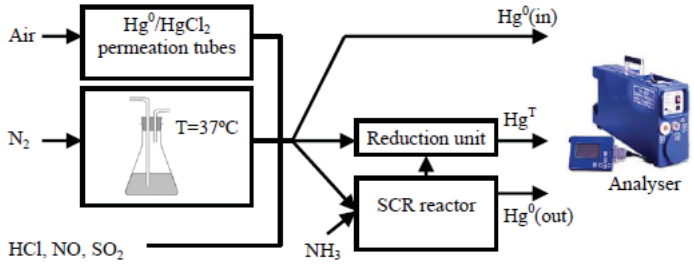

Figure 17. Schematic Drawing of Laboratory Setup

All tubing in contact with mercury consists of pyrex glass, which is heated to 140ºC to avoid precipitates and adsorption on the surfaces. Hg^0 or $HgCl_2$ is introduced into the gas via VICI Metronics Dynacal® Permeation devices. H_2O is added by passing part of the gas through a bubble-flask with H_2O at 37ºC. The remaining gas components HCl, NO, NH_3, SO_2, O_2 and N_2, are added from gas bottles. The simulated flue gas in this study contains the concentrations given in Table 1.

Component	Concentration
Hg^0	2.5-25 µg/Nm³
$HgCl_2$	17-53 µg/Nm³
O_2	4 %(vol)
H_2O	5 %(vol)
HCl	2.5-55 ppm
NH_3	0-350 ppm
NO	0-350 ppm

Table 1: Composition of the Simulated Flue Gas

The reactor consists of pyrex glass and contains a single monolithic SCR channel in fixed dimensions. Experiments across the channel are run isothermally with a temperature profile of +/- 2ºC.

Mercury is analysed in the Lumex RA-915+ analyser, which uses cold vapour atomic absorption spectrometry to measure gaseous elemental mercury Hg^0 continuously.

The reduction unit serves the purpose of reducing all $HgCl_2$ in the gas stream to Hg^0, which enables a total mercury measurement (HgT) with the analyser that only detects Hg^0.

Testing Procedure: Fresh SCR catalysts are initially preconditioned over night at T=350ºC in a gas flow containing 20 µg/Nm³ Hg^0, 4 ppm HCl, 5% O_2, 2% H_2O, 50 ppm NO and NH_3 in balance N_2. SCR catalysts have a capacity for mercury adsorption in an amount that is very dependent on the gas composition and temperature. The preconditioning serves the purpose of saturating the catalyst with adsorbed mercury under conditions that are similar to the experiments.

The conversion (X) of Hg^0 to Hg^{2+} over the SCR is measured for different operating conditions, gas compositions and catalyst types. The steady-state conversion over the SCR is calculated as

$$X = \frac{\left[Hg^0\right]^{in} - \left[Hg^0\right]^{out}}{\left[Hg^0\right]^{in}}$$

The calculation presupposes that all Hg^0 disappearing over the SCR has been oxidized to Hg^{2+}, which only will be true at steady-state, where no sorption phenomena are occurring. Various measures have been carried out to ensure this. The initial preconditioning of the catalyst minimizes sorption transients between experiments and each set of testing conditions have stabilized for minimum 1 hour before the measurement. Experiments where larger changes are imposed on the test conditions are left over night to stabilize.

Total mercury measurements can confirm steady-state operation if Hg^T(in)=Hg^T(out), but since operation of the reduction unit is very time consuming, Hg^T measurements have only been performed for experiments with $HgCl_2$ as the mercury source. Alternatively, the repeatability of measurements for experiments with Hg^0 as the mercury source has been validated across three different test days and two different catalysts, which has validated the testing procedure.

The range of conditions tested is given in Table 2

.

Catalyst	
Vanadia content	Low, typical, high
Operating conditions	
Flow [NL/h]	82-250, 500
Temperature [ºC]	250-450

Table 2: Range of Operating Conditions

Results and Discussion

The study consists of two separate parts:

1. Experiments performed at a very low flow rate: U=82 NL/h. The objective of the experiments is to examine the 'equilibrium speciation' of mercury that exists after long SCR reactors in the presence of NH_3. The given flow rate is so low that sufficient contact time between the gas and catalysts is achieved and no changes in speciation are observed by further decreasing the flow rate. These experiments will show the maximum mercury oxidation that can be achieved over SCR catalysts for different gas compositions and operating temperatures. This speciation will be referred to as the 'stabilized speciation', since (as will be shown) it differs from the thermodynamic equilibrium speciation of mercury.

2. Experiments performed at a very high flow rate: U=500 NL/h. The objective of this study is to pinpoint what effects from the DeNOx reaction that actually influence the kinetics of the Hg^0 oxidation over SCR catalysts under different operating temperatures.

Studying the 'stabilized' mercury speciation in the presence of NH_3

Plotted in Figure 18 is the fraction of $HgCl_2$ at the SCR outlet at T=350ºC as function of the flow rate for three different gas compositions:

1) 1.3 ppm HCl and no NH_3,

2) 1.3 ppm HCl and 80 ppm NH_3, and

3) no HCl and 80 ppm NH_3.

The gas contains no NO, so the NH_3 concentration will be constant across the SCR. Tests have been performed for either 100% Hg^0 at the SCR inlet or 100% $HgCl_2$. The simulated flue gas otherwise contains 4% O_2 and 2.5% H_2O in balance N_2.

Data show that in the absence of NH_3, all mercury leaving the SCR will approach 100% $HgCl_2$ for decreasing flows for even very low HCl=1.3 ppm. In the absence of HCl, all mercury leaving the SCR is Hg^0 in the entire range of flows tested regardless of Hg^0 or $HgCl_2$ is at the inlet.

Both these observation are in line with thermodynamic predictions for the mercury speciation at 350ºC. The results also confirm that both oxidation of Hg^0 and reduction of $HgCl_2$ can take place over the SCR catalyst. Reference tests over an empty SCR reactor (i.e. without catalyst) show only minor change in mercury speciation supporting that both these reactions are catalytically induced.

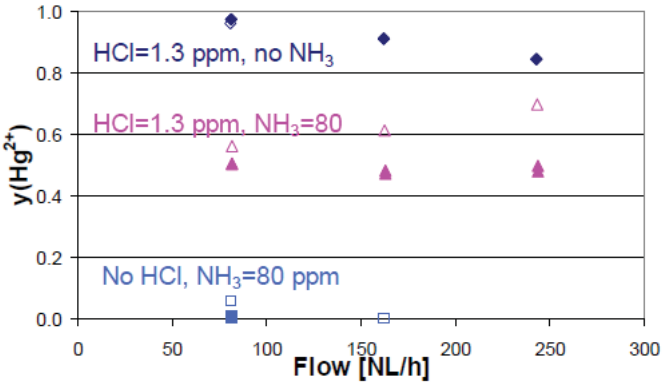

Figure 18. The fraction of $HgCl_2$ after the SCR at T=350ºC as function of the flow rate. The gas contains Hg^0 or $HgCl_2$ in 4% O_2 and 2.5% H_2O in balance N_2. Closed brackets: Hg^0 at inlet, open brackets: $HgCl_2$ at inlet.

In the presence of both HCl and NH_3, the mercury speciation will approach the same speciation (~53% $HgCl_2$) with either Hg^0 or $HgCl_2$ at the SCR inlet for decreasing flows. According to global thermodynamic calculations using software from HSC, there is no difference in the thermodynamic equilibrium speciation of mercury in the absence/presence of NH_3 for the given simulated flue gas. Thermodynamic predictions suggest that all mercury should exist as $HgCl_2$ under the given conditions. This shows that the 'stabilized' mercury speciation after the SCR does not coincide with the thermodynamic equilibrium and that the presence of NH_3 promotes the reduction of $HgCl_2$ to Hg^0.

The stabilized mercury speciation is approached asymptotically for decreasing flows over the SCR, but appears to have been reached +/- 5% at 82 NL/h. All further measurements of the 'stabilized' mercury speciation are therefore performed at this flow rate. Also, only Hg^0 is used as mercury source.

Plotted in Figure 19 (page 22) is the 'stabilized' mercury speciation after the SCR as function of temperature for different NH_3 concentrations. The simulated flue gas otherwise contains 25 µg/Nm³ Hg^0, 2.5 ppm HCl, 4% O_2, 5% H_2O in balance N_2.

The mercury speciation at temperatures below 300ºC is com-

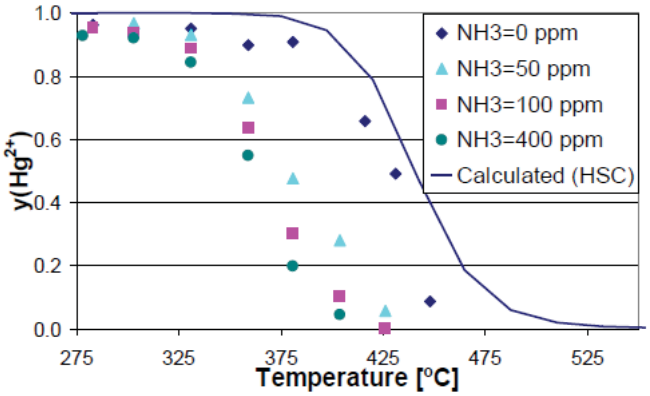

Figure 19. The fraction of $HgCl_2$ after the SCR at U=82 NL/h as function of temperature. The gas contains 25 µg/Nm³ Hg^0, 2.5ppm HCl, 4% O_2 and 5% H_2O in balance N_2. The calculated thermodynamic equilibrium for HCl=2.5 ppm is shown in the full line.

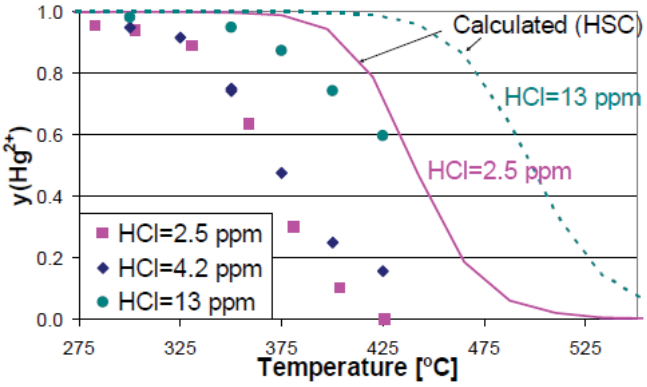

Figure 20. The fraction of $HgCl_2$ after the SCR at U=82 NL/h as function of temperature. The gas contains 25 µg/Nm³ Hg^0, 100 ppm NH_3, 4% O_2 and 5% H_2O in balance N_2. The calculated thermodynamic equilibrium for HCl=2.5 ppm and 13 ppm are shown in full and dotted lines, respectively.

pletely shifted towards $HgCl_2$ at all NH_3 concentrations. At T=325ºC and above, the speciation gradually shifts towards Hg^0. In the absence of NH_3, the 'stabilized' mercury speciation is close to thermodynamic predictions, which supports the validity of the experimental measurements.

In the presence of NH_3, the 'stabilized' mercury speciation shifts towards Hg^0 at a lower temperature. At T=425ºC, all mercury exists as Hg^0 in the presence of NH_3 down to 50 ppm. This shows that at very low HCl=2.5 ppm, no Hg^0 oxidation can be expected over an SCR operated at elevated temperatures until most of the NH_3 has been consumed in the DeNOx reaction.

Plotted in Figure 20 is the 'stabilized' mercury speciation after the SCR as function of temperature for different HCl concentrations.

The simulated flue gas otherwise contains 25 µg/Nm³ Hg^0, 100 ppm NH_3, 4% O_2, 5% H_2O in balance N_2. The experimental results show that the 'stabilized' mercury speciation is shifted towards $HgCl_2$, when the HCl concentration is increased from 2.3 to 13 ppm.

Discussion part #1: Hypothesis of pseudo-equilibrium

The presented results show that the assumption of a global thermodynamic equilibrium does not hold for mercury chemistry in flue gases. The realized mercury speciation will rather be a result of a number of mercury reactions running at a considerable rate. It is here proposed that it is the relative rate of such oxidizing and reducing reactions that determine the 'stabilized' mercury speciation over the SCR catalyst.

The presence of NH_3 has been shown to promote the reduction of $HgCl_2$ to Hg^0, so the two net reactions taking place over the SCR catalyst could be:

$$\mathbf{R1:\ 2\ HCl + Hg^0 + ½\ O_2 \leftrightarrow HgCl_2 + H_2O}$$

$$\mathbf{R2:\ 2\ NH_3 + 3\ HgCl_2 \leftrightarrow N_2 + 3\ Hg^0 + 6\ HCl}$$

Both reactions are completely shifted to the right according to thermodynamics at relevant SCR operating temperatures. The forward reactions will therefore be prevalent for each reaction.

Mercury is present in flue gases in a factor 1000 less than HCl, NH_3, O_2 and H_2O, so neither of these two reactions will impose changes in the concentration of these components.

This means that both reaction R1 and R2 can be running simultaneously and only influence the mercury speciation.

When the rates of reaction R1 and R1 are identical, the effect on the mercury speciation is cancelled out, which is seen by the sum of the two reactions. By this hypothesis, the experimental observations can now be explained as follows:

- For the case with 100% Hg^0 at the SCR inlet, the rate of reaction R1 will dominate at the beginning of the catalyst, but as the concentration of $HgCl_2$ increases, so will the rate of reaction R2.

- At a given mercury speciation, the rates of reaction R1 and R2 have become identical and the mercury speciation will remain unchanged for the rest of the catalyst.

- The stabilized mercury speciation is, hence, not a thermodynamic equilibrium, but can be considered as a dynamic equilibrium caused by the two reactions, i.e. a pseudo-equilibrium.

The pseudo-equilibrium mercury speciation, where the two reaction rates are identical, is influenced by concentrations of NH_3 and HCl and by the SCR operating temperature.

Experiments have been performed to examine the effect of the catalyst composition on the pseudo-equilibrium mercury speciation. Results are not shown here, but the data demonstrate that increasing vanadia-concentration increases the relative rate of reaction R1 to reaction R2. This means that the speciation is shifted towards more $HgCl_2$ for increasing vanadia content in the catalyst.

Studying the effect of NH_3 and NO on the kinetics of the Hg^0 oxidation

Experiments are now performed at a very high flow rate, which does not give enough time for the mercury speciation to stabilize over the SCR, but instead enables a study of the kinetics of the Hg^0 oxidation over SCR catalysts.

The laboratory tests are performed at a very high linear velocity v=10.8 Nm/s and on a monolithic catalyst with a low hydraulic diameter (dh=3.4 mm) in order to minimize the resistance to external mass transfer and thus enhance the differences in surface reactivity across different testing conditions. In this context, it should be noted that the Hg^0 oxidation in these experiments will not represent what can be expected over full-scale reactors.

The objective of this study is to identify the relevant mechanisms in connection with the DeNOx reaction that influence the Hg^0 oxidation at different operating temperatures. The following three net reactions will be shown to be relevant for the catalytic oxidation of Hg^0 in the presence of both NO and NH_3.

$$\mathbf{R1:\ 2\ HCl + Hg^0 + \tfrac{1}{2}\ O_2 \leftrightarrow HgCl_2 + H_2O}$$

$$\mathbf{R2:\ 2\ NH_3 + 3\ HgCl_2 \leftrightarrow N_2 + 3\ Hg^0 + 6\ HCl}$$

$$\mathbf{R3:\ 2\ NO + 2\ NH_3 + \tfrac{1}{2}\ O_2 \leftrightarrow 2\ N_2 + 3\ H_2O}$$

Reaction R1 is the oxidation of Hg^0 with HCl, reaction R2 is the reduction of $HgCl_2$ with NH_3 and reaction R3 is the DeNOx reaction.

Plotted in Figure 21 (page 24) is the steady-state conversion of Hg^0 over the SCR as function of temperature for three different gas compositions:

1) 4.2 ppm HCl,
2) 4.2 ppm HCl and 100 ppm NH_3, and
3) 4.2 ppm HCl and 100 ppm NH_3 and NO.

The simulated flue gas otherwise contains 4-12.5 $\mu g/Nm^3$ Hg^0, 4% O_2, 5% H_2O in balance N_2.

In the absence of NO and NH_3, only reaction R1 takes place. It is seen that the Hg^0 oxidation is constant at a level of 82 % in the temperature range 250-350ºC. The low temperature dependence indicates that sorption phenomena play a major role for the kinetics of the catalytic Hg^0 oxidation via reaction R1, since both reaction rate constants and rates of mass transfer will increase with temperature. For temperatures above 350ºC, the Hg^0 oxidation starts decreasing, since the thermodynamic equilibrium is approached and the reverse of reaction R1 is becoming important.

The experiment has been repeated for HCl=46 ppm (data not shown), where the same Hg^0 oxidation (82%) is achieved for 250-350ºC. This suggests that the adsorption of Hg^0 limits the rate of the catalytic reaction R1 and not the adsorption of HCl.

In the presence of NH_3 with/without NO, a maximum Hg^0 oxidation is seen around 300ºC. Interestingly, the results suggests that a synergistic inhibition between NO and NH_3 is taking place, since the inhibition is greater than for NH_3 alone in the temperature range 250-375ºC. Such synergism could suggest that the DeNOx reaction influences the mercury chemistry on SCR catalysts.

Two different mechanistic regimes of the kinetics of the Hg^0 oxidation appear to exist under DeNOx-conditions: Below T=300ºC and above T=350ºC. The temperature region T=300-350ºC represent a mixed regime.

- For temperatures above 350ºC, the overall Hg^0 oxidation is approaching the pseudo-equilibrium speciation, when NH_3 is present. The plotted pseudo-equilibrium represents the upper level of $HgCl_2$ that can be achieved for HCl=4.2 ppm and

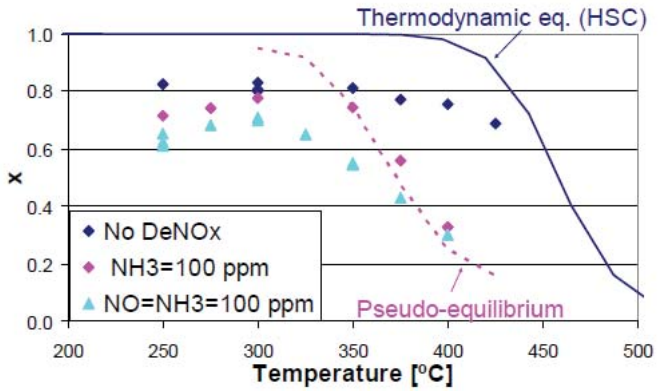

Figure 21. The conversion of Hg^0 over the SCR at U=500 NL/h as function of temperature. The gas contains 4-12.5 µg/Nm^3 Hg^0, 4.2 ppm HCl, 4% O_2 and 5% H_2O in balance N_2. The thermodynamic equilibrium for HCl=4.2 ppm is shown in full line. The pseudo-equilibrium for HCl=4.2 ppm and NH_3=100 ppm is shown in dotted line.

NH_3=100 ppm. This shows that the 'stabilized'mercury speciation over the SCR is reached very fast for T>375ºC. The mercury speciation after the SCR will then greatly depend on how the NH_3 concentration evolves in the reactor.

- The synergistic inhibition by NO and NH_3 is seen in the entire temperature region until the effect is obliterated by the $HgCl_2$ reduction at temperatures above T=375ºC.

- For temperatures below 300ºC, the presence of NH_3 alone has an increasing inhibition on the Hg^0 oxidation with decreasing temperature. This cannot be due to $HgCl_2$ reduction via reaction R2.

Discussion part #2: Hypothesis of Lewis sites being active in the Hg^0 oxidation

Vanadia has been shown to be the active specie for the catalytic Hg^0 oxidation on commercial SCR catalysts. Based on the experimental data, it is now hypothesized that the surface Lewis sites (V^{5+}=0) are active sites for the catalytic Hg^0 oxidation.

Two possible explanations for the inhibiting effects under DeNOx conditions at low temperatures support the hypothesis:

- Effect of NH_3 alone below 300ºC: Nova et al. (2006) demonstrates an inhibiting effect of NH_3 on the DeNOx reaction at low temperatures, since NH_3 in addition to adsorbing on Brønsted sites on the catalyst also adsorb on Lewis sites at low temperatures. This unspecific adsorption blocks active sites on the catalyst and thus inhibits the DeNOx reaction. The same phenomena would inhibit the catalytic Hg^0 oxidation if Lewis sites are active sites for this reaction as well.

- Synergistic effect with NO and NH_3: The mechanism for the DeNOx reaction involves the reduction of active Lewis (V^{5+}=0) sites that needs to be oxidized to regain activity:

$$2\ V^{4+}\text{-}OH + \tfrac{1}{2}\ O_2 \leftrightarrow 2\ V^{5+}{=}O + H_2O$$

Lietti et al. (1996) reports that the kinetics of the DeNOx reaction is inhibited by the reoxidation of Lewis sites at low temperatures. The synergistic inhibition by NO and NH_3 on the catalytic Hg^0 oxidation can reasonably be explained by a consumption of active Lewis in the DeNOx reaction.

Effect of HCl in the different temperature regimes

The following experiments are performed in order to validate that different mechanisms are causing an inhibition by the DeNOx reaction on the Hg^0 oxidation at low and at high temperature.

Plotted in Figure 22 (page 25) is the conversion of Hg^0 over the SCR as function of HCl at T=250ºC and T=350ºC. The simulated flue gas contains 4.2-12.2 µg/Nm^3 Hg^0, 100 ppm NO and NH_3, 4% O_2, 5% H_2O in balance N_2.

For T=350ºC, the Hg^0 oxidation increases with increasing HCl up to 17 ppm. The maximum Hg^0 oxidation is just slightly below the level seen in the absence of NO and NH_3. It has been demonstrated in the first part of this study that increasing HCl increases the relative rate of the Hg^0 oxidation (R1) to the $HgCl_2$ reduction (R2). Reaction R2 takes place at T>325ºC and so the promoting effect of HCl can be explained by the latter.

For T=250ºC, only a minor promotion by increasing HCl is seen for the Hg^0 oxidation that continues to be at a much lower level than in the absence of NO and NH_3. Data in this study has suggested that Hg^0 adsorption governs the kinetics

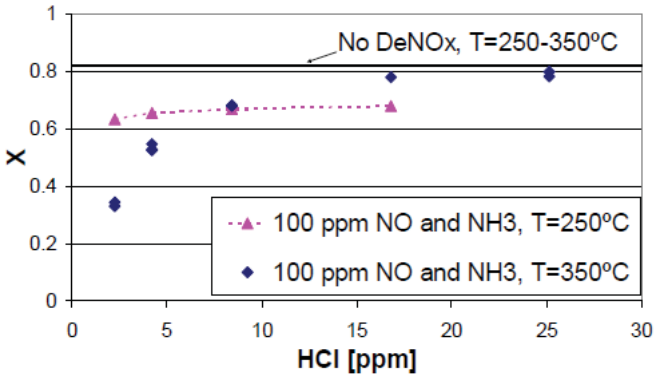

Figure 22. The conversion of Hg^0 over the SCR at U=500 NL/h as function of HCl. The gas contains 4.2-12.2 µg/Nm^3 Hg^0, 100 ppm NO and NH_3, 4% O_2 and 5% H_2O in balance N_2. The exp. measured conversion of Hg^0 in the absence of DeNOx is ~82% for in the range: T=250-350ºC and HCl=4.2-46 ppm. This is shown in full line.

of the catalytic Hg^0 oxidation via reaction R1. If Hg^0 adsorption on Lewis sites is limiting the overall rate of reaction R1, then increasing the concentration of HCl will not influence the reaction rate.

Conclusions

The Hg^0 oxidation over commercial SCR catalysts in the presence of the DeNOx reaction has been studied via laboratory experiments.

This study demonstrates that different mechanistic regimes exist for the kinetics of the Hg^0 oxidation at relevant SCR operating temperatures. This means that the effect of various parameters (e.g. HCl) can be different, when operating in each of these regimes.

NH_3 alone inhibits the Hg^0 oxidation by two different mechanisms:

- At T>325ºC, $HgCl_2$ reduction by NH_3 (reaction R2) will take place. The observed Hg^0 oxidation will reflect the relative rate of the Hg^0 oxidation via reaction R1 and the $HgCl_2$ reduction via reaction R2. The effect of reaction R2 can be dampened by increasing HCl or increasing vanadia-content on the catalyst.

- At T<300ºC, NH_3 will adsorb on active Lewis sites on the catalyst and make them unavailable for Hg^0 adsorption. Increasing the vanadia-content on the catalyst will increase the number of active sites for Hg^0 adsorption. Notice that increasing HCl above 4.2 ppm will not improve the Hg^0 oxidation.

The combination of NO and NH_3 serves a synergistic inhibition on the Hg^0 oxidation by the consumption of active Lewis sites in the DeNOx reaction. The effect is evident in the temperature range 250-375ºC. Above this temperature, the synergistic effect is obliterated due to the $HgCl_2$ reduction via reaction R2 dominating the mercury speciation.

This study point at the following means for improving the Hg^0 oxidation over commercial SCR reactors in the entire temperature range

- Increase the vanadia-content of catalyst. This should be done while still keeping the SO_3 production low.

- Add an additional catalyst layer, so the concentrations of NO and NH_3 are negligible at the final catalyst layer. In the absence of NO and NH_3, the surface reactivity of current commercial SCR catalysts for Hg^0 oxidation is sufficiently high, so the overall rate of the catalytic Hg^0 oxidation is primarily limited by external mass transfer, when operating at industrially relevant operating conditions (v~2 Nm/s, higher hydraulic diameter).

As a final comment: Notice that the space velocity for the given laboratory experiments is substantially higher than for full-scale SCR operation. This means that the reported conversions of Hg^0 are lower than, and do not represent full-scale conversions.

HALDOR TOPSOE
CATALYZING YOUR BUSINESS

For further information contact:

***Karin Madsen**, Haldor Topsoe A/S, kama@topsoe.dk*

Karin Madsen works as a research engineer in the R&D Environmental Department at Haldor Topsøe A/S. She has carried out an industrial PhD-project in collaboration between Haldor Topsøe A/S and the Technical University of Denmark on Mercury oxidation over SCR catalysts.

WPCA Corporate Sponsors

WPCA Chairman / Secretary
Paul Ford, President
Redkoh Industries
300 Valley Road, Hillsborough, NJ 08844 USA
Email: paul.ford@redkoh.com

WPCA Treasurer
Robert Mudry, President
Airflow Sciences Corporation
12190 Hubbard Street
Livonia, MI 48150-1737 USA
Email: rmudry@airflowsciences.com

WPCA Vice President
Cindy Khalaf, President
Johnson Matthey Catalysts LLC
1121 Alderman Drive Suite 204
Alpharetta, GA 30005 USA
Email: cindy.khalaf@jmusa.com

Greg Bielawski, Mgr. Environ. Aftermarket;
Babcock & Wilcox
20 S. Van Buren Avenue,
Barberton, OH 44203 USA
Email: gtbielawski@babcock.com

Tony Licata, Vice President
Babcock Power Inc.
5 Neponset Street
Worcester, MA 01606-2714 USA
Email: tlicata@babcockpower.com

Allen Kephart, Senior Vice President
Clean Air Engineering
1601 Parkway View Drive
Pittsburgh, PA 15205 USA
Email: akephart@cleanair.com

Mark Ehrnschwender, Dir. Bus. Management
Steag Energy Services LLC
304 Linwood Road, Suite 102
Kings Mountain, NC 28086 USA
Email: mark.ehrnschwender@steag.us

Tom Lugar, President
Fisher-Klosterman/Buell APC
200 North 7th Street, Ste 2
Lebanon, PA 17046 USA
Email: twl@fkinc.com

Tim Stark, Applications Engineer
GE Environmental
47 Solana Road
Ponte Vedra Beach, FL 32082 USA
Email: robert.taylor@ge.com

Nate White, Dir. Business Development
Haldor Topsoe, Inc.
5510 Morris Hunt Drive
Fort Mill, SC 29708 USA
Email: tnw@topsoe.com

Tae Young Lee, President
KC Cottrell
160-1 Tongkyo-dong, Mapo-gu
Seoul, 121-817 South Korea
Email: tylee@kc-cottrell.com

Jerry VanDerWerff, Nat. Sales Manager
Sorb-N-Ject; Nol-Tec Systems, Inc.
425 Apollo Drive
Lino Lakes, MN 55014 USA
Email: JerryVanDerWerff@nol-tec.com

Susan Reinhold, CEO
Reinhold Environmental Ltd.
3850 Bordeaux Drive, Northbrook, IL 60062 USA
Email: sreinhold@reinholdenvironmental.com

James Reynolds, VP Wet ESP Technology
Siemens Environ. Systems and Services
501 Grant Street, Pittsburgh, PA 15219-4429 USA
Email: jamesreynolds@siemens.com

Michael Hatsfelt, General Manager
Southern Environmental, Inc.
6690 West Nine Mile Road
Pensacola, FL 32526 USA
Email: mhatsfelt@sei-group.com

Royce Warnick, Dir. Environ. Controls
Stock Equipment Company
16490 Chillicothe Road
Chagrin Falls, OH 44023 USA
Email: royce.warnick@stockequipment.com

Gordon Maller, Bus. Development Mgr.
URS Corporation
2935 Thousand Oaks Drive
Austin, TX 78746 USA
Email: gordon_maller@urscorp.com

Bill Hankins, VP Sales, U2A Systems
Wahlco
2722 South Fairview
Santa Ana, CA 92704 USA
Email: bhankins@wahlco.com

Bob Cardell, President
MET
200 North 7th STreet
Lebanon, PA 17046 USA
Email: bcardell@met.net

Curt Biehn, Mgr Technical Sales & Mkt
Mississippi Lime Company
3870 S. Lindbergh Blvd., St. Louis, MO 63127
Email: crbiehn@mississippilime.com

Jamie Fessenden, Bus. Mgr. Emission Control Tech
Norit-Americas
3200 University Ave., Marshall, TX 75670 USA
Email: jfessenden@norit-americas.com

WPCA Officers

WPCA President
Melanie McCoy
General Manager
Wyandotte Municipal Service

WPCA Vice President
Doug Hartman
Supervisor Environ. Performance
FirstEnergy

WPCA Advisors

Melissa Allen, System Engineer
TVA

Greg Betenson, Principal Engineer
PacifiCorp

Jim Chaney
Environmental Controls Specialist
Ameren Generation

Joseph Hantz,
Manager, Environmental Services
Entergy

Michael Olive,
Mgr, Major Project Integration
Progress Energy Florida

Ebrahim Patel, Senior Consultant - APC
ESKOM-GTD

Bruce Salisbury, Mechanical Engineer
Arizona Public Service

John Walker
Senior Engineer - Station Electrical
Duke Energy

Scott Williams, Senior Engineer
Duke Energy

Juergen Wirling, Senior Manager
Rheinbraun Brennstoff GmbH